Available online at www.sciencedirect.com
ScienceDirect
Geochimica et Cosmochimica Acta 74 (2010) 4078–4096
Geochimica et Cosmochimica Acta
www.elsevier.com/locate/gca

Copper isotopic zonation in the Northparkes porphyry Cu–Au deposit, SE Australia

Weiqiang Li [a,*], Simon E. Jackson [a,b], Norman J. Pearson [a], Stuart Graham [a]

[a] GEMOC ARC National Key Centre, Department of Earth and Planetary Sciences, Macquarie University, NSW 2109, Australia
[b] Geological Survey of Canada, Natural Resources Canada, 601 Booth Street, Ottawa, Ont., Canada K1A 0E8

Received 3 December 2009; accepted in revised form 2 April 2010; available online 8 April 2010

Abstract

Significant, systematic Cu isotopic variations have been found in the Northparkes porphyry Cu–Au deposit, NSW, Australia, which is an orthomagmatic porphyry Cu deposit. Copper isotope ratios have been measured in sulfide minerals (chalcopyrite and bornite) by both solution and laser ablation multi-collector inductively coupled plasma-mass spectrometry (MC-ICP-MS). The results from both methods show a variation in δ^{65}Cu of hypogene sulfide minerals of greater than 1‰ (relative to NIST976). Significantly, the results from four drill holes through two separate ore bodies show strikingly similar patterns of Cu isotope variation. The patterns are characterized by a sharp down-hole decrease from up to 0.8‰ (0.29 ± 0.56‰, 1σ, $n = 20$) in the low-grade peripheral alteration zones (phyllic–propylitic alteration zone) to a low of ~−0.4‰ (-0.25 ± 0.36‰, 1σ, $n = 30$) at the margins of the most mineralized zones (Cu grade >1 wt%). In the high-grade cores of the systems, the compositions are more consistent at around 0.2‰ (0.19 ± 0.14‰, 1σ, $n = 40$). The Cu isotopic zonation may be explained by isotope fractionation of Cu between vapor, solution and sulfides at high temperature, during boiling and sulfide precipitation processes. Sulfur isotopes also show an isotopically light shell at the margins of the high-grade ore zones, but these are displaced from the low δ^{65}Cu shells, such that there is no correlation between the Cu and S isotope signatures. Fe isotope data do not show any discernable variation along the drill core. This work demonstrates that Cu isotopes show a large response to high-temperature porphyry mineralizing processes, and that they may act as a vector to buried mineralization.

1. INTRODUCTION

Two fundamental goals of mineral deposit research are to identify the metal source and to understand the processes that have mobilized, transported and deposited the metals. Geochemists have applied a number of isotopic systems, including light stable isotopes (e.g., H, O and S) and radiogenic isotopes (e.g., Nd, Pb and Os), to trace the metal(s) source in mineral deposits and to unravel the mineralization processes (e.g., Sheppard and Gustafson, 1976; Rye, 1993; Farmer and DePaolo, 1997; Mathur et al., 2000). Yet, the stable isotope ratios of the metals themselves (e.g., Fe, Cu and Zn) can potentially provide the most direct answers to the longstanding questions on the source of the metals and mineralization processes in ore-forming systems. Copper has received the greatest attention among researchers interested in applying metal stable isotope to mineral deposits. Copper has two stable isotopes with the isotopic ratio commonly expressed in δ notation ($\delta^{65}Cu = (R_{sample}/R_{NIST976} - 1) \times 1000$ where $R = {}^{65}Cu/{}^{63}Cu$). The first attempts to measure Cu isotope ratios of natural samples were made a half century ago using TIMS (Walker et al., 1958; Shields et al., 1965), but not until the last decade, with the development of MC-ICP-MS (Walder et al., 1993; Walder, 1997; Halliday et al., 1998), did routine high precision measurement of metal stable isotopes became possible.

* Corresponding author. Present address: Department of Geoscience, University of Wisconsin-Madison, 1215 W. Dayton Street, Madison, WI 53706, USA. Tel.: +1 6087727385.
E-mail address: liweiq@gmail.com (W. Li).

0016-7037/$ - see front matter © 2010 Elsevier Ltd. All rights reserved.
doi:10.1016/j.gca.2010.04.003

Maréchal et al. (1999) were the first to detail analytical techniques for high precision measurement of Cu isotopes with MC-ICP-MS. Following on from that study, Cu isotopes have been applied to a wide spectrum of hydrothermal systems (Fig. 1), including modern black smokers (Zhu et al., 2000; Rouxel et al., 2004), massive sulfide (Mason et al., 2005), porphyry (Graham et al., 2004; Mathur et al., 2005, 2009), skarn (Graham et al., 2004; Maher and Larson, 2007) and other hydrothermal ore deposits (Jiang et al., 2002; Larson et al., 2003; Markl et al., 2006).

Despite the variety of the mineralizing systems that have been investigated, there are some common features of the Cu isotope signatures, including: (1) δ^{65}Cu values of Cu-bearing minerals cluster around zero ($\delta^{65}Cu \approx 0$); (2) the variation in Cu isotope ratios in most mineralizing systems is larger than 1‰, which is more than 10 times larger than the analytical uncertainty that can be achieved for Cu isotope ratios by MC-ICP-MS and (3) mineralizing systems influenced by low-temperature redox processes show much larger variation in Cu isotope ratios than the high-temperature mineralizing systems (Fig. 1).

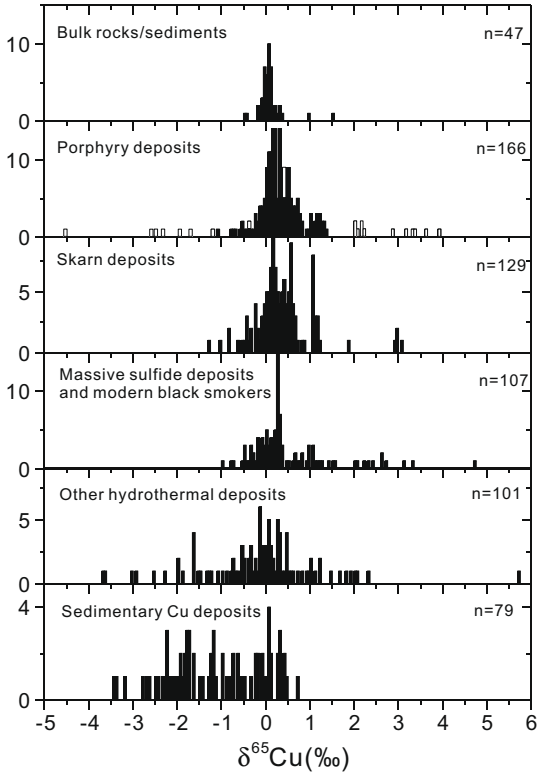

Fig. 1. Compilation of Cu isotope data from rocks/sediments (Maréchal et al., 1999; Archer and Vance, 2004; Rouxel et al., 2004; Li et al., 2009) and from various hydrothermal mineralizing systems: porphyry deposits (Larson et al., 2003; Graham et al., 2004; Mathur et al., 2005, 2009; Asael et al., 2007), skarn deposits (Larson et al., 2003; Graham et al., 2004; Maher and Larson, 2007), volcanogenic massive sulfide deposits and modern black smokers (Zhu et al., 2000; Rouxel et al., 2004; Mason et al., 2005), other hydrothermal deposits (low-temperature hydrothermal vein-type copper deposit, Jiang et al., 2002; Michigan native copper deposits, Larson et al., 2003; Schwarzwald mining district, Markl et al., 2006) and sedimentary Cu deposits (Asael et al., 2007). Note that the unfilled bars in the histogram for porphyry deposits are data of oxidized ores as reported by Mathur et al. (2009) and some extreme data of oxidized ores in that study are not plotted due to scale restriction.

It is becoming clear that redox processes at low temperature can produce significant Cu isotope fractionation, as shown by various laboratory experiments (Zhu et al., 2002; Ehrlich et al., 2004; Mathur et al., 2005; Asael et al., 2006; Fernandez and Borrok, 2009; Kimball et al., 2009) and studies on Cu-bearing samples from supergene environments (e.g., Rouxel et al., 2004; Markl et al., 2006; Asael et al., 2007; Mathur et al., 2009) and stream waters (Borrok et al., 2008; Kimball et al., 2009). However, the implications of the published Cu isotope data in high-temperature mineralization systems remain unclear. In particular, there is no consensus on whether Cu isotopes bear useful information for interpretation of mineralization processes. For example, Graham et al. (2004) carried out an in situ laser ablation MC-ICP-MS study of the Grasberg Cu–Au deposit. The authors observed a significant range in the δ^{65}Cu value of chalcopyrite (from 0.02‰ to 1.34‰) and found that an increase in the δ^{65}Cu value is associated with the three successive intrusions of the Grasberg Igneous Complex. This work implies that significant Cu isotope fractionation occurs at high temperature. By contrast, high-temperature hydrothermal processes in the Schwarzwald mining district in southern Germany did not produce significant Cu isotopic variations; instead, the majority of the variation in Cu isotope signatures reflect low-temperature processes and associated redox reactions (Markl et al., 2006).

To further examine whether significant, systematic Cu isotopic variations exist in high-temperature hydrothermal mineralizing systems and to explore the possible mechanisms accounting for the Cu isotope variations reported from high-temperature mineral deposits, we have carried out a detailed and systematic investigation of the Cu isotopic compositions of sulfide minerals from the Northparkes porphyry deposit in SE Australia. Iron and S isotope ratios of sulfides from the deposit were also measured. The Northparkes district was selected because it contains several well-preserved, small-scale, orthomagmatic porphyry orebodies with well documented geology, regular zonation of mineralization grade, mineralogy and associated alteration assemblages, and because an earlier exploratory study of one deposit had demonstrated systematic spatial trends in Cu isotope ratios (Graham et al., 2002). It thus provides an excellent location to investigate the behavior of Cu isotopes in high-temperature hydrothermal systems.

2. GEOLOGICAL BACKGROUND AND SAMPLES

The Northparkes porphyry Cu–Au deposit (also named the Goonumbla porphyry Cu deposit in earlier literature) is located in the mid-west of New South Wales, Australia. The deposit is hosted within the Ordovician Goonumbla Volcanic Complex, situated in the eastern Lachlan Fold Belt (Simpson et al., 2005). The Goonumbla Volcanic Complex is part of the Junee-Narromine Volcanic Belt, one of five Ordovician to Silurian volcanic belts that make up

the Paleozoic Lachlan Fold Belt in SE Australia (Fig. 2A). Eleven porphyry systems have been identified at Northparkes. The four exploitable orebodies at Northparkes (E22, E26, E27 and E48, Fig. 2B) had a combined ore reserve of 131.7 Mt at 1.2 wt% Cu and 0.5 g/t Au (data in 2001, Lickfold et al., 2003).

The Northparkes deposits belong to the magmatic end member of the porphyry deposit spectrum (Lickfold et al., 2003). Mineralization at Northparkes has a close spatial association with shoshonitic magmatism, the source of which is interpreted, based on elemental geochemistry and Sr–Nd–Pb isotope signatures, to be the product of high-pressure fractionation of mantle-derived magmas (Heithersay and Walshe, 1995). The age of the mineralization is constrained between 446 and 437 Ma by $^{40}Ar/^{39}Ar$ dating of biotite and sericite (Perkins et al., 1990; Lickfold et al., 2003) and U–Pb SHRIMP dating of zircon from intrusions (Perkins et al., 1990; Butera et al., 2001). Several fluid inclusion studies suggest that the main stage quartz were precipitated from a high-temperature (>350 ℃), high salinity (>40 wt% NaCl equiv.) hydrothermal fluid released from the porphyry intrusions (Heithersay and Walshe, 1995; Lickfold et al., 2003). The initial $\delta^{34}S$ value of the hydrothermal fluid was estimated to be −1.5‰ (Heithersay and Walshe, 1995). H and O isotopic signatures suggest that both the central potassic alteration core and the main stage phyllic alteration zone of the deposit are of primary magmatic origin (Harris and Golding, 2002).

Despite the Ordovician–Silurian age, the Northparkes deposits are well preserved. The area has undergone only weak metamorphism, with the occasional occurrence of zeolite to lower greenschist minerals in some rocks (Suppel et al., 1998). The weathering and oxidation of the deposit is variable but generally not significant and the thickness of the fully and partially oxidized ore zones are less than 35 m (Jones, 1985; Heithersay et al., 1990). There is a sharp transition between the oxidation zone and the primary ore zone. Accordingly, the supergene enrichment of Cu and Au is limited, as secondary chalcocite blankets are a few meters thick or not developed (Jones, 1985). The samples selected for this study were taken from drill cores at depth greater than 100 m are all free of oxidation.

As porphyry deposits are generally complex in their geology and genesis, two separate porphyry systems (E26 and E48) were investigated to assess the reproducibility of any Cu isotopic variations. Chalcopyrite grains from one drill core (E26D46) have been analyzed using LA-MC-ICP-MS in a previous reconnaissance industry research project (Graham et al., 2002) and the Cu and Fe isotope results are used in this study. Some of these samples were re-analyzed. New samples were taken from diamond drill core E26D76 that intersects the E26 orebody from a different direction than the drill core E26D46. The angle between the projected traces of the two drill holes on plan view is near perpendicular (Fig. 2C). The same sampling strategy was also applied to the E48 orebody. Two drill cores (E48D13 and E48D20), which intersect the E48 orebody from different directions, were sampled; the projected traces of the two drill cores on plan view is near perpendicular as well (Fig. 2D). This sampling strategy was designed to optimize the representativeness of the samples and to build a spatial framework that is vital for interpretation of Cu isotope data. The diamond drill cores investigated in this study have a diameter of about 4 cm, with length varying from several hundred meters to over one thousand meters. The drill cores were sampled at intervals of approximately 25 m, where possible. Sixty samples (15 from E26D76, 6 from E26D46, 20 from E48D13 and 19 from E48D20) were analyzed. There is profound variation in lithology of host rock, alteration style, veining and mineral assemblage among samples. Brief descriptions of these features for each sample are given in Electronic Annex EA-1.

The E26 orebody is the largest orebody in the Northparkes district. It is a stockwork pipe with a vertical extent of over 900 m (Fig. 2E). The host rock of the E26 orebody is a unit of the Ordovician Goonumbla Volcanic Complex named the Wombin Volcanics. The quartz stockwork is centered on two subvertical quartz monzonite porphyry intrusions, named QMP1 and QMP2 (Heithersay and Walshe, 1995). The main Cu mineralization is associated with QMP1-related stockwork quartz veining and alteration. QMP2 was emplaced after QMP1 and generally diluted or destroyed the earlier Cu mineralization especially at the QMP1–QMP2 contact, although parts of QMP2 are mineralized (Fig. 2E). Sulfides occur in veins, fractures and as disseminations. There is an overall zonation of sulfides in the E26 ore body from a bornite ± chalcocite-dominant core to a chalcopyrite-dominant shell and a pyrite-dominant peripheral zone. Zones of alteration are centered on the porphyry intrusions, with the intensity of the alteration diminishing outwards. The central zone of pervasive K-feldspar alteration generally correlates with the bulk of mineralization (>1.0% Cu). The K-feldspar alteration zone grades outward to a biotite–K-feldspar subzone and into a propylitic alteration zone at the periphery. The boundary between the biotite–K-feldspar subzone and the propylitic alteration zone corresponds approximately to the 0.3% Cu contour (e.g., Heithersay et al., 1990; Heithersay and Walshe, 1995). The alteration pattern of the E26 ore body is broadly consistent with the classic model for porphyry systems (Lowell and Guilbert, 1970) except that the phyllic alteration does not occur between K-feldspar alteration zone and propylitic alteration zone. Phyllic alteration locally overprints K-feldspar alteration and is generally controlled by fractures.

The E48 deposit is the second largest of the Northparkes Cu–Au ore bodies and is located ~1.5 km north of E26 and approximately midway between E26 and E27 (Fig. 2B). The host rock of E48 is also the Wombin Volcanics. Narrow (up to 50–60 m), pencil-like monzonite porphyries intrude all units of the volcanic sequence from the E31 stock to the top of the sequence (Fig. 2F). Mineralization occurs in veins, fractures and as disseminations and is closely associated with the porphyry intrusions. Sulfide mineralogy is zoned around the intrusions, varying from bornite-dominant in the core zone to chalcopyrite and then pyrite dominant in the peripheral zones. Alteration is also centered on the quartz monzonite porphyry intrusions with intensity decreasing outwards. However, the alteration pattern is less clear than the E26 orebody. Biotite–magnetite (BMT) alter-

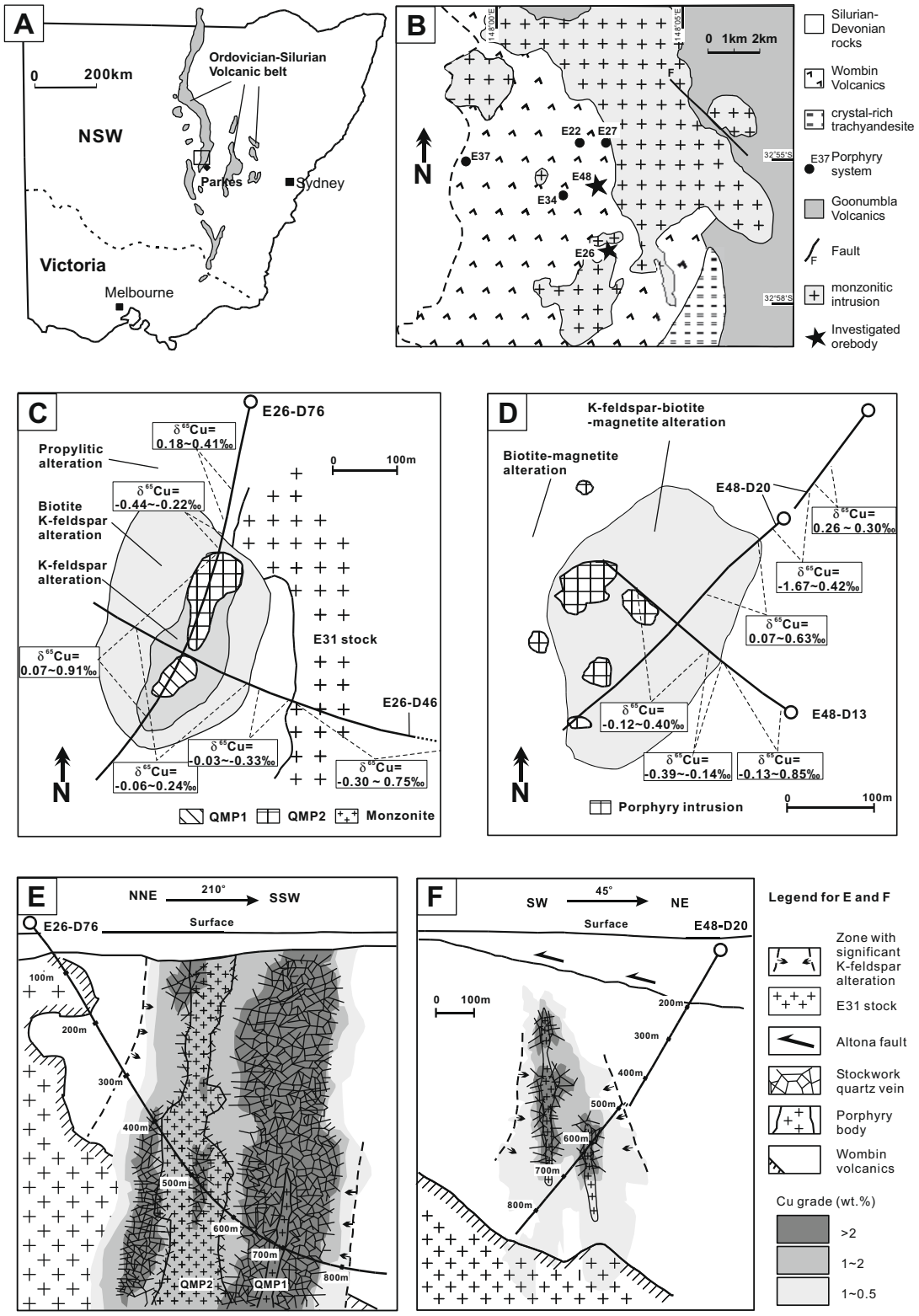

Fig. 2. Geology of the Northparkes Cu–Au porphyry deposit. (A and B) Geological setting of the Northparkes Cu–Au porphyry deposit. (C and D) Geology and alteration of the E26 (C) and E48 (D) orebodies at the 10,000 RL level (approximately at a depth of 300 m), showing the projections of drill holes that were analyzed in this study. Cu isotope data obtained from the four cores are summarized in (C) and (D). Panel C is modified from Heithersay et al. (1990), panel D is made from interpretation of 3D block models from the Northparkes Mines and logging data. (E and F) Cross sections through the E26 (E) and E48 (F) orebody at Northparkes. Made from interpretation of 3D block models from the Northparkes Mines and logging data.

ation is generally associated with peripheral mineralization where Cu grade is below 0.5 wt%. In the core of the system, where Cu grade is above 0.5 wt%, the alteration is dominated by assemblages of K-feldspar–biotite–magnetite (KBM), hematite–sericite–carbonate (HSC), fault–quartz sericite–pyrite (FQS) and sericite–carbonate–albite or white sericite wash (WSW).

3. ANALYTICAL PROCEDURES

In order to discern possible small-scale isotopic heterogeneity (e.g., Rouxel et al., 2004) and retain spatial information of the isotope data, two in situ analytical approaches were used in this study: (1) sampling of sulfides by microdrilling followed by digestion of the drilled minerals to make Cu solutions for isotopic analysis and (2) in situ sampling of the sulfides by laser ablation. Laser ablation produces an aerosol that can be directly introduced into a MC-ICP-MS for isotopic analysis. Solution analysis of transition metal isotopes is a mature method; however, it is more time consuming and lacks the spatial resolution of laser ablation analysis. Laser ablation transition metal isotope analysis, while offering superior spatial resolution and being more time effective, is much less frequently reported in the literature and its application to the study of mineral deposits has not been fully exploited. In this study, both methods are used, with some sulfide grains analyzed by both methods to confirm the accuracy of LA-MC-ICP-MS technique.

3.1. Micro-milling and Cu isotope measurement by solution MC-ICP-MS

The polished blocks made from drill core samples were washed firstly in ethanol and then de-ionized water in an ultrasonic bath to remove dust before being mounted onto a New Wave Research Micro-mill for micro-sampling. Prior to milling, a drop of Milli-Q water (5–10 μL) was placed onto the surface of the sulfide grain of interest with a micropipette, to lubricate the drill bit and collect the fine sample dust as a slurry. After milling, the slurry was immediately transferred into a Teflon beaker with a micropipette. To increase sample recovery, the crater was refilled with Milli-Q water that was pipetted into the Teflon beaker; the process was repeated. After that, the crater was examined under a reflected light microscope to check that the hole was contained within a single sulfide phase. If a different sulfide was identified in the crater to that exposed at the surface, the milled material was discarded to eliminate contamination from sulfide intergrowth. The micro-milling technique has been described in detail by Charlier et al. (2006).

The depth of milling was set between 150 and 200 μm. The crater milled with this setting has a diameter of approximately 100 μm at the surface and the mass of material milled is estimated to be 1–2 μg. The size of the sulfide grains selected in this study was generally larger than 200 μm, which enabled two or more craters to be milled in each grain. In general, two millings produced enough material for Cu isotope measurement.

After micro-milling, each sulfide slurry was digested in 100 μL double-distilled concentrated HNO_3 in a sealed Teflon beaker at 80 °C overnight, then evaporated to dryness at 80 °C. The sample was subsequently dissolved in 2 ml 2% HNO_3. Ten percent of each solution was diluted and scanned on an Agilent 7500cs ICP-MS to determine the concentration of Cu and any other matrix elements. Except for Fe, the concentrations of other matrix elements, including W which came from the tungsten carbide drill bit of the micro-mill, were negligible compared with Cu. A number of previous studies have assessed the matrix effect of Fe on Cu isotope measurement and demonstrated that measured Cu isotope ratios are not affected by Fe contents, even when the Fe/Cu ratio is up to 15 (Zhu et al., 2000; Graham et al., 2004; Rouxel et al., 2004; Markl et al., 2006; Maher and Larson, 2007). Based on the results from previous studies, the influence of Fe on the Cu isotope measurements in this study is considered to be negligible as chalcopyrite, bornite and chalcocite have stoichiometric Fe/Cu ratios of 1/1, 1/5 and 0, respectively. Additionally, the polyatomic interferences of S on ^{65}Cu (e.g., $^{32}S^{33}S^{+}$, $^{33}S^{16}O_2^{+}$) were found to be negligible based on the measured signals at a.m.u. 64. Rouxel et al. (2004) also showed the effect of S on $^{65}Cu/^{63}Cu$ measurement to be undetectable. Thus ion exchange chromatography was not applied to purify the solutions and a matrix matched standard was not used. To prepare the solutions for Cu isotope measurement on the MC-ICP-MS, they were diluted to 300 ppb Cu in 2% HNO_3 doped with 1.2 ppm Ni (NIST SRM 986). Any matrix effects induced by this relatively high Ni content, required because of the low isotopic abundance of ^{62}Ni (ca. 3.6%), are corrected via normalization to the correct isotopic ratio of the Ni (Li et al., 2009).

The solutions were analyzed on a Nu Plasma MC-ICP-MS (Nu034) in the "wet-plasma" mode without using a membrane desolvation sample introduction system at the GEMOC National Key Centre, Macquarie University. The details of the instrument settings and analytical protocols can be found in Electronic Annex EA-2-I and a previous paper (Li et al., 2009). The standard error of the $^{65}Cu/^{63}Cu$ ratio for each analysis was mostly smaller than 0.04‰. The long-term reproducibility of the Cu isotope measurements based on 105 analyses of an in-house Cu standard used in the analytical protocol was 0.09‰ (2σ).

3.2. Cu and Fe isotope measurement by LA-MC-ICP-MS

In situ Cu isotopic measurement by laser ablation (LA)-MC-ICP-MS was carried out on chalcopyrite grains in polished blocks. The LA system was a New Wave Research UP213 operated with an in-house built sample cell, which was coupled to a Nu Plasma MC-ICP-MS (Nu005). A Nu Instruments DSN-100 membrane desolvation system was used to mix into the sample carrier gas stream (He) an aerosol of NIST SRM 986 Ni (Ar) for mass bias correction. The set up of the system is schematically shown in Electronic Annex EA-2-IIa), and the operating conditions of the LA-MC-ICP-MS system are listed in Electronic Annex EA-2-IIb. A sample chalcopyrite grain and a chalcopyrite standard were analyzed alternately using the same

ablation conditions. Data were acquired and corrected for mass bias using the time resolved analysis (TRA) software of the Nu Plasma instrument. The certified $^{62}Ni/^{60}Ni$ ratio for NIST SRM 986 and the exponential mass bias law were used.

To correct for isotopic fractionation induced by laser sampling processes (e.g., Jackson and Günther, 2003; Kühn et al., 2007), the mass bias-corrected Cu isotope ratios were further corrected off-line by application of the sample-standard bracketing procedure. The sample-standard bracketing technique works only when the analytical system runs under exactly the same condition for both sample and standard. For isotopic measurement using LA-MC-ICP-MS, laser operating conditions, the composition and ablation behavior of the sulfides and the transportation efficiency of the aerosols all contribute to the degree of isotopic fractionation. Procedures used to minimize differences in these parameters included: (1) the lower part of the laser ablation cell was rotated to move the sulfide of interest to the gas inlet–outlet axis of the cell prior to each measurement to ensure matching of gas dynamics for samples and standard in the cell; (2) both sample and standard were ablated for the same time (3 min), except for occasional thin sulfide grains, to minimize the ablation time-dependence of the isotopic fractionation and (3) a natural hydrothermal chalcopyrite from the Bougainville porphyry copper Cu deposit was used as the standard for LA-MC-ICP-MS measurement of chalcopyrite as close matching of sample and standard is vital for in situ Cu isotope measurement by laser ablation (Ikehata et al., 2008). Other Cu-bearing minerals (bornite and chalcocite) were not analyzed by LA-MC-ICP-MS, as appropriate standards for those minerals were not available.

The Bougainville chalcopyrite standard was selected following a laser ablation survey, which found it to be exceptional isotopically homogenous. The isotopic difference between 19 equally spaced analyses on different parts of the chalcopyrite standard is smaller than the internal analytical precision (Fig. 3A). The $\delta^{65}Cu$ value of the chalcopyrite standard, measured by solution MC-ICP-MS (Nu034), is $-0.81\pm0.10‰$ (2σ, $n = 8$). Using this standard, the LA-MC-ICP-MS technique is sufficiently precise for the purpose of distinguishing Cu isotopic variations in hydrothermal deposits (Fig. 3B). The accuracy of the Cu isotope data obtained by the laser ablation technique in this work and in the study of Graham et al. (2002) has been verified by re-analyzing some sulfide grains by solution MC-ICP-MS following micro-mill sampling. There is excellent consistency between the two sets of data over a large span of Cu isotopic compositions (Fig. 3C). This also confirms the accuracy of Cu isotope data in the paper of Graham et al. (2004).

The procedures used for Fe isotopic analysis by LA-MC-ICP-MS have been described by Graham et al. (2004).

3.3. S isotope measurement

The sulfur isotopic composition of selected sulfides in samples from drill cores E26D76 and E48D20 was measured at the Centre for Isotope Studies at CSIRO, North Ryde, NSW, Australia. Samples were collected by micro-milling as described in Section 3.1. Sulfur isotope measurement requires a larger sample size than for Cu isotopic analyses. Therefore, larger milling depth, multiple millings and rastering of the sulfide grain were applied. In this study, sulfide grains that had been milled for Cu isotope measurement but had sufficient material remaining for S isotope measurement were selected.

Sulfide samples (tens to hundreds of μg) were combusted in a tin cup using a modified Roboprep elemental analyzer attached to a Finnigan 252 mass spectrometer. Samples were analyzed relative to an internal gas standard and laboratory standards, Ag_2S-3 ($\delta^{34}S = +0.4‰$ VCDT) and CSIRO-S-SO_4 ($\delta^{34}S = +20.4‰$ VCDT). The laboratory standards have been calibrated using international standards IAEA-S1 ($\delta^{34}S = -0.3‰$ VCDT) and NBS-127 ($\delta^{34}S = +20.3‰$ VCDT). Replicate analyses of sulfide standards are within $\pm0.2‰$.

4. RESULTS

Results of Cu, Fe and S isotope measurements, together with a brief description of the samples, are presented in the tables in Electronic Annex EA-1. Note that the Cu isotope compositions of chalcopyrite from drill core E48D20 and E26D46 were determined by LA-MC-ICP-MS, and the data reported are the averages (±2 standard deviations) of the multiple analyses of different grains on the same sample. The solution MC-ICP-MS data are the averages (±2 standard deviations) of multiple analyses of the same solutions. The original results of individual laser ablation measurements are tabulated in Electronic Annex EA-3. The solution MC-ICP-MS data of selected sulfides that have been analyzed by LA-ICP-MS are provided in Electronic Annex EA-2-IIc. The variation in the isotopic values, Cu grade and alteration assemblages with depth for the four drill holes (E26D76, E26D46, E48D20 and E48D13) are plotted in Figs. 4a, b and 5a, b, respectively. The data for Cu grade and alteration assemblages of the drill cores are taken from internal reports of Northparkes Mines and are not tabulated here.

4.1. Cu isotope results

Copper isotope ratios from the two drill cores from the E26 orebody show significant variation (>1‰) and similar spatial variations with ore grade and alteration zone (Fig. 4). In drill core E26D76, the $\delta^{65}Cu$ values of most sulfides from the center of the orebody (Cu grade up to >1 wt%, with drill core depth between 425 m and 750 m) cluster around 0.2‰ ($0.21 \pm 0.10‰$, 1σ, $n = 12$) except for one sample (0.46‰ and 0.91‰, E26D76-500 m), and there is no difference between Cu isotope compositions of sulfides hosted in QMP1 and QMP2. This zone is dominated by K-feldspar alteration. At the margin of the orebody, where the Cu grade starts to decrease outward (core depths between 325 m and 375 m) and alteration changes to biotite–K-feldspar alteration overprinted locally by phyllic alteration, $\delta^{65}Cu$ values of the sulfides drop to around $-0.4‰$ ($-0.35 \pm 0.09‰$, 1σ, $n = 5$). Outside this zone (core

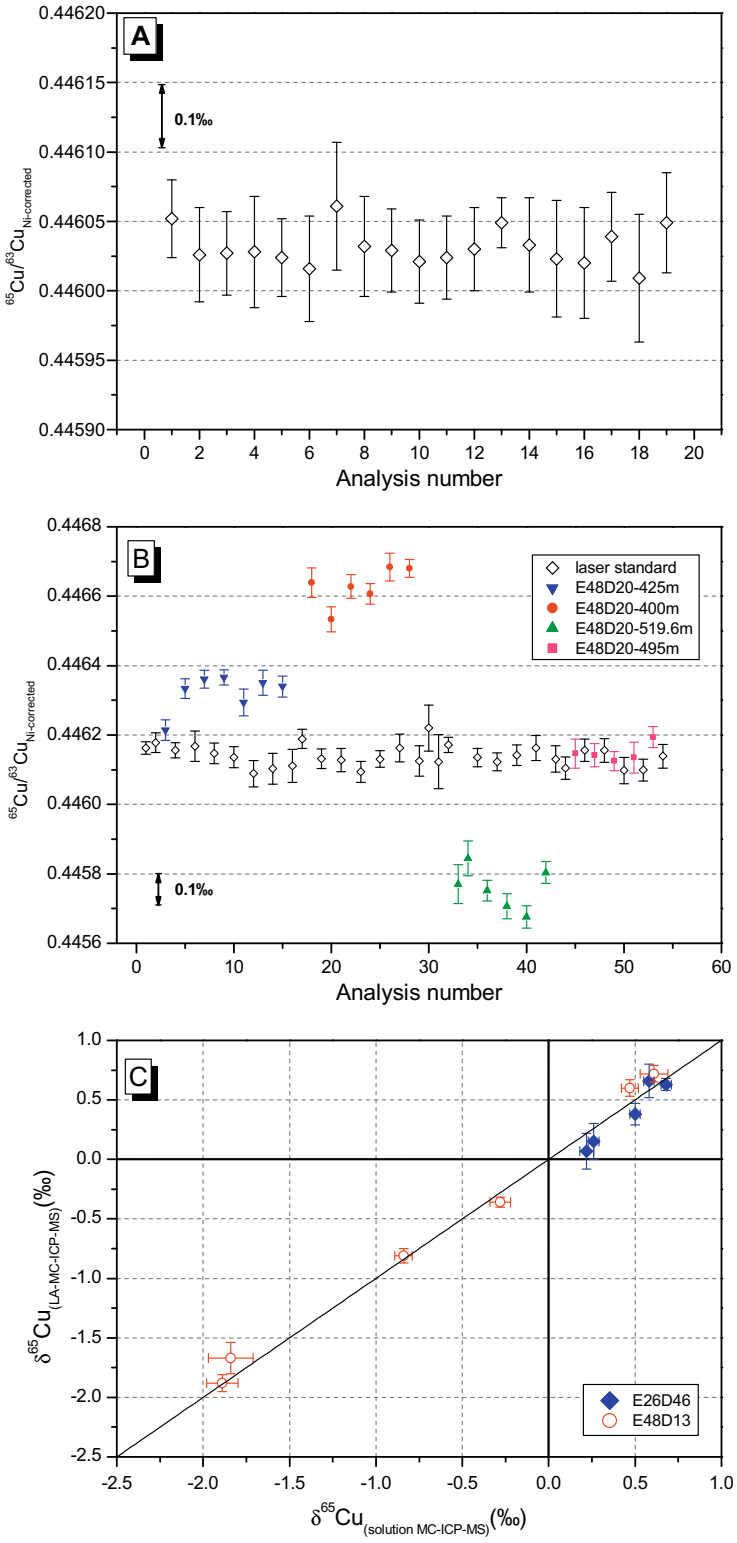

Fig. 3. (A) Diagram demonstrating the Cu isotopic homogeneity of the Bougainville chalcopyrite standard. Nineteen spot analyses were performed evenly over the 1.5 cm × 1.5 cm area of chalcopyrite. Error bars denote two standard errors for each analysis. The reproducibility (2σ) of the 19 analyses is 0.06‰ in $\delta^{65}Cu$. (B) Diagram showing the Cu isotopic data obtained by LA-MC-ICP-MS in one analytical session. The variability of the $\delta^{65}Cu$ values for the laser standard is 0.14‰ (2σ, $n = 30$). The larger variation may be caused by opening and closing of the laser ablation cell to change samples, which affected the stability of the LA-MC-ICP-MS system. Error bars denote two standard errors for each analysis. (C) Comparison of the Cu isotope data measured by LA-MC-ICP-MS and solution MC-ICP-MS. LA-MC-ICP-MS data from drill core E26D46 were determined in a previous study (Graham et al., 2002); other solution and laser ablation data were obtained in this study.

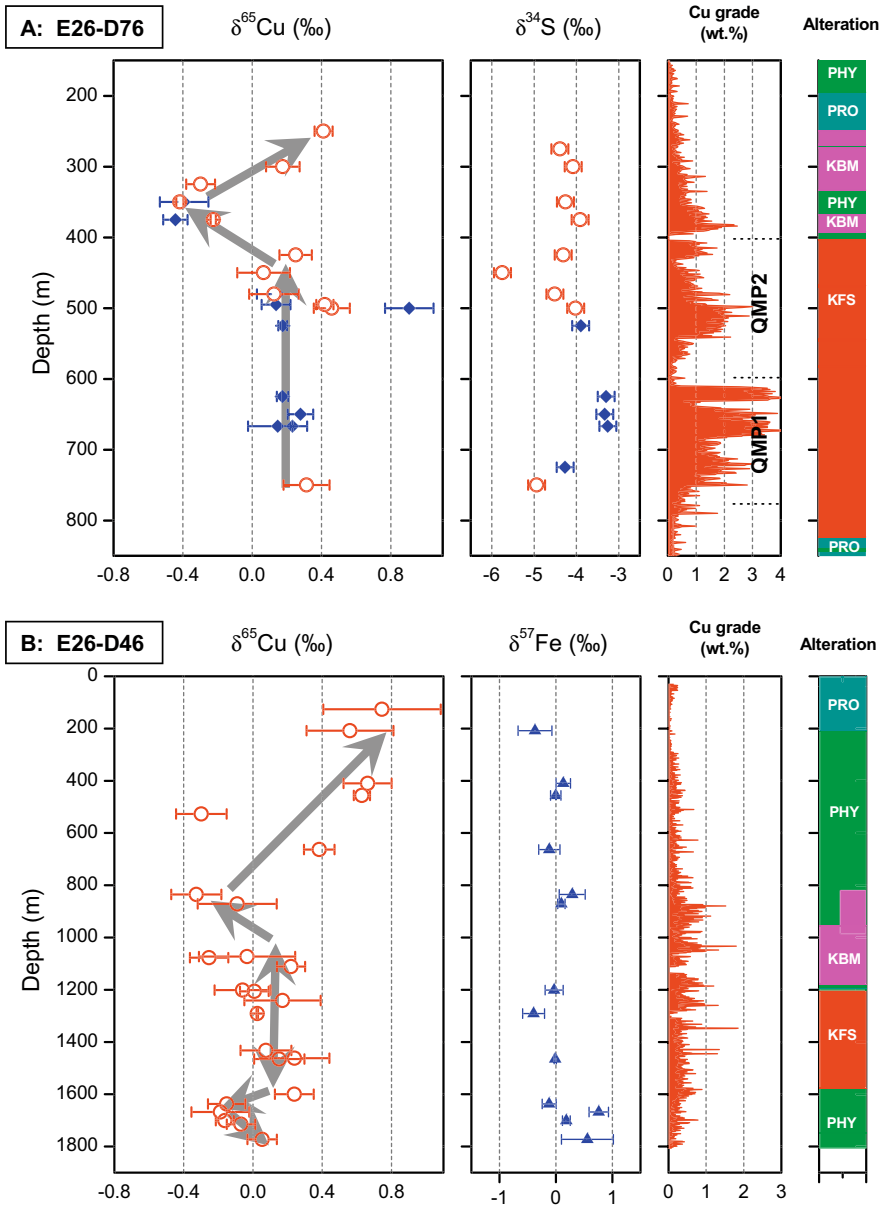

Fig. 4. Variation of Cu isotope and S (or Fe) isotope compositions of bornite (solid diamond) and chalcopyrite (circle), Cu grade, and alteration assemblage with depth along drill cores E26D76 (3A) and E26D46 (3B). Error bars denote two standard deviations of multiple analyses. Alteration types are denoted with abbreviations and colored bands. PHY, phyllic alteration; PRO, propylitic alteration; KBM, biotite–K-feldspar alteration; KFS, K-feldspar alteration. The trend of Cu isotope variation is denoted by the gray arrows in the background.

depth < 300 m), the δ^{65}Cu values of the sulfides increase to 0.4‰.

The laser ablation data from drill core E26D46, which cuts through the orebody from another direction, show a similar pattern of variation. From a core depth of 126 m to 835 m, where the Cu grade is below 0.3 wt% and alteration changes from outermost propylitic alteration to phyllic alteration and biotite–K-feldspar alteration inwards, the average δ^{65}Cu values of chalcopyrite decrease from 0.75‰ to as low as −0.33‰. The δ^{65}Cu values increase to around 0.1‰ (0.12 ± 0.11‰, 1σ, $n = 9$) for drill core samples between core depths of 1111 m and 1600 m, which represent the center of the orebody with typical K-feldspar alteration and Cu grades >0.5 wt% on average. For samples from core depths greater than 1600 m, which are again from the phyllic alteration zone at the margin of the high-grade Cu core of the system, the δ^{65}Cu values of chalcopyrite decrease again to values as low as −0.19‰.

The pattern of Cu isotope variation from the E48 orebody is consistent with that of the E26 orebody (Fig. 5). In drill core E48D13, the δ^{65}Cu values of the sulfides decrease from 0.85‰ at a core depth of 451 m to −0.39‰ at a depth of 675 m, with the negative values occurring in samples from the margin of the orebody where the Cu grades increase sharply inwards from less than 1 wt% to more than 1 wt% and the dominant alteration changes from

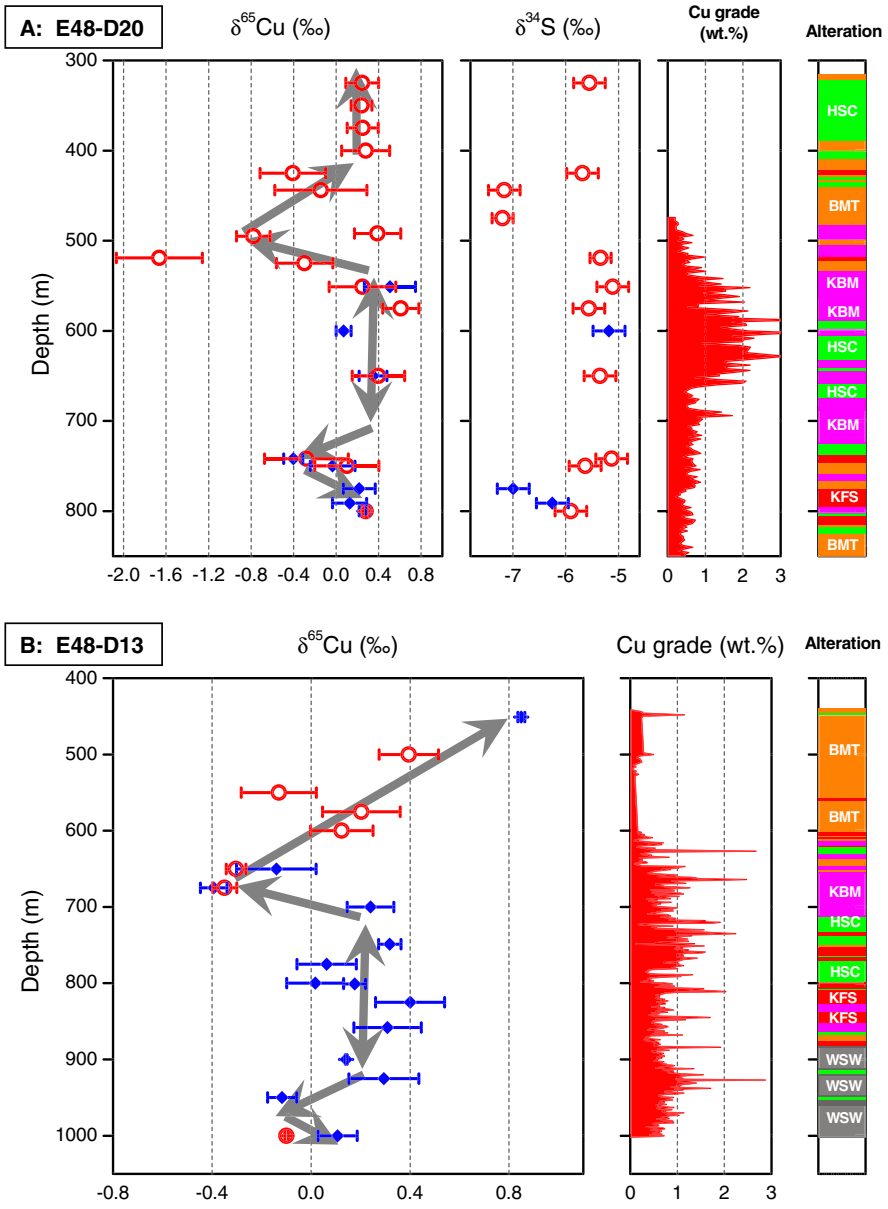

Fig. 5. Variation of Cu (and S) isotopic compositions of bornite (solid diamond) and chalcopyrite (circle), Cu grade and alteration assemblage with depth along drill cores E48D20 (Fig. 4A) and E48D13 (Fig. 4B). Error bars denote two standard deviations of multiple analyses. Alteration types are denoted with abbreviations and colored bands. HSC, hematite–sericite–carbonate alteration; BMT, biotite–magnetite alteration; KBM, biotite–K-feldspar alteration; KFS, K-feldspar alteration. The trend of Cu isotope variation is denoted by the gray arrows in the background. (For interpretation of the references to colour in this figure legend, the reader is referred to the web version of this article.)

biotite–magnetite alteration to K-feldspar–biotite–magnetite alteration. Samples from the most intensely mineralized part of the orebody (at core depths between 700 m and 925 m) show δ^{65}Cu values clustering around 0.20‰ (0.16 ± 0.14‰, 1σ, $n = 14$). Alteration in this part of the core includes K-feldspar–biotite–magnetite, hematite–sericite–carbonate, K-feldspar and white sericite wash (sericite–carbonate–albite) alteration. Beneath a core depth of 925 m, where the drill hole emerges from the high-grade core of the system, there seems to be a decrease in δ^{65}Cu, with two samples out of four analyzed having Cu isotope compositions below or equal to −0.10‰.

The Cu isotopic data from drill hole E48D20, measured mainly by LA-MC-ICP-MS, also show a similar pattern, with shifts to negative δ^{65}Cu values at the margins of the orebody. Chalcopyrite from samples in the peripheral biotite–magnetite alteration zone (core depth range of 325 m and 400 m) have δ^{65}Cu around 0.30‰ (0.28 ± 0.02‰, 1σ, $n = 4$), whereas samples between 425 m and 525 m, where Cu grades increase to >0.5% and the dominant alteration changes to K-feldspar–biotite–magnetite alteration, mostly have lighter Cu isotopic composition (-0.47 ± 0.70‰, 1σ, $n = 6$). Notably, sample E48D20-519.6 m has the lowest δ^{65}Cu value (−1.67‰) measured from the Northparkes

deposit. The δ^{65}Cu values of samples from the center of the ore body (with core depth between 551 m and 650 m) vary between 0.07‰ and 0.63‰ (0.35 ± 0.20‰, 1σ, $n = 5$). The Cu isotope composition of the sulfides show another drop to negative values at a core depth of 742 m, as Cu grades decline, before rising back to around 0.2‰ at greater depth. From 700 m to 750 m, the dominant alteration assemblage changes from K-feldspar–biotite–magnetite to biotite–magnetite.

To summarize, the data from four drill cores from two separate orebodies suggest that there is significant and systematic zonation of Cu isotopes in the two porphyry systems of the Northparkes district. Copper isotope data from the center of the orebodies (Cu grade >0.5–1 wt%) are generally between 0.0‰ and 0.4‰ (0.19 ± 0.14‰, 1σ, $n = 40$), whereas Cu isotope data from the margins of the orebodies, where Cu grades decrease rapidly and alteration assemblages change outward from K-feldspar-bearing to phyllic and biotite–magnetite, are mostly around −0.4–0.0‰ (-0.25 ± 0.36‰, 1σ, $n = 30$). Copper isotope data from rocks peripheral to the orebodies, dominated by biotite–magnetite and propylitic assemblages, generally vary from 0.2‰ to 0.8‰ (0.29 ± 0.56‰, 1σ, $n = 20$). Thus, although there is some difference in alteration styles between the E26 and E48 porphyry systems, the light Cu isotopic zones (δ^{65}Cu ≈ −0.4–0‰) approximately correlate with the outward margin of K-feldspar alteration.

4.2. S isotope results

The S isotope ratios were measured for samples from two drill cores, E26D46 and E48D20. The δ^{34}S values of bornite from the center of the E26 orebody varies between −3.3‰ and −4.3‰. The S isotope data of chalcopyrite from the same drill core is slightly but systematically lower, varying between −3.9‰ and −5.8‰, with the majority of data clustering around −4.1‰. There seems to be excursions to more negative δ^{34}S values at core depths of about 470 m and at greater than 650 m. Neither of these zones coincides with the zone of negative δ^{65}Cu values. Otherwise, there is no systematic trend to the S isotope data in drill core E26D46.

In general, the S isotope compositions of sulfides in drill core E48D20 are isotopically lighter than those from E26D46, with the majority of data around −5.5‰. There seems to be a decrease in δ^{34}S value for samples from core depths between 425 m and 500 m and for samples deeper than 750 m. These two excursions to more negative values do not coincide with the zones of negative δ^{65}Cu values but occur immediately outside them. Overall, the range of the S isotope data obtained in this study is consistent with those of previous studies on the Northparkes deposit (Jones, 1991; Heithersay and Walshe, 1995; Howland-Rose, 1996; Lickfold, 2002).

5. DISCUSSION

5.1. Cu isotopic variability in porphyry Cu deposits

The range of δ^{65}Cu values for sulfide minerals from the Northparkes deposit is between −1.67‰ and 0.91‰, but the majority of the data lie between −0.40‰ and 0.60‰. The variation in δ^{65}Cu at Northparkes is more than 10 times the external analytical precision of the Cu isotope measurements and, while not surprising given our current knowledge of Cu isotopes (Fig. 1), requires explanation.

The patterns of Cu isotope variation shown by our data are unlikely to be a coincidental artifact of random fluctuation of Cu isotope ratios in the orebodies. Four drill cores cutting across two separate orebodies from different directions show the same general data pattern (Figs. 4 and 5). The isotopic variation amongst samples from the center of each orebody is smaller than the isotopic difference between samples from the center and the margin of the orebody. Furthermore, although specimen-scale Cu isotope heterogeneity in some samples has been revealed by LA-MC-ICP-MS (Fig. 3B and Electronic Annex EA-3), the magnitude of the heterogeneity is generally of second order compared to the isotopic variation on the orebody scale; i.e., most of the samples do not show significant Cu isotopic heterogeneity (Figs. 4B, 5A and Electronic Annexes EA-1, EA-3).

Co-existence of sulfides (e.g., bornite and chalcopyrite, or chalcocite and bornite) is common, especially in the cores of the orebodies (Electronic Annex EA-1). The Cu isotope data for the different sulfide minerals within a sample were measured wherever possible, and the results are plotted in Fig. 6. The plot shows that, for most samples, the Cu isotopic difference between bornite and chalcopyrite is less that ±0.2‰. This is not consistent with the findings of two previous studies that suggested that bornite in equilibrium with chalcopyrite may be isotopically lighter by about 0.4‰ in δ^{65}Cu (Larson et al., 2003; Maher and Larson, 2007). This discrepancy may be due to the higher ore-forming temperature in the Northparkes deposit compared to the deposits studied in the two previous investigations. For the chalcocite–bornite pair, three out of five points are close to the line of no inter-mineral Cu isotopic fractionation. To summarize, the inter-mineral Cu isotopic fractionation is also of second order compared to the isotopic variation on the orebody scale.

5.2. Cause of Cu isotope variation in high-temperature hydrothermal systems

Variation in Cu isotopic signatures of sulfides in hydrothermal deposits may be the result of either variation of the Cu isotopic composition of the source(s), or fractionation of Cu isotopes during the ore-forming processes (mobilization, transport and deposition), or a combination of the two. The possible mechanisms accounting for the isotopic variations in the Northparkes porphyry systems are discussed below.

5.2.1. Source heterogeneity of hydrothermal fluids

There are two fundamental sources of Cu in porphyry deposits: the magma of the porphyry intrusion and the host rock (Hedenquist and Lowenstern, 1994). In both of the Northparkes porphyry systems, as the zone of isotopically light Cu is sandwiched by the isotopically heavier core (porphyry intrusion) and the strata of the Wombin Volcanics, it

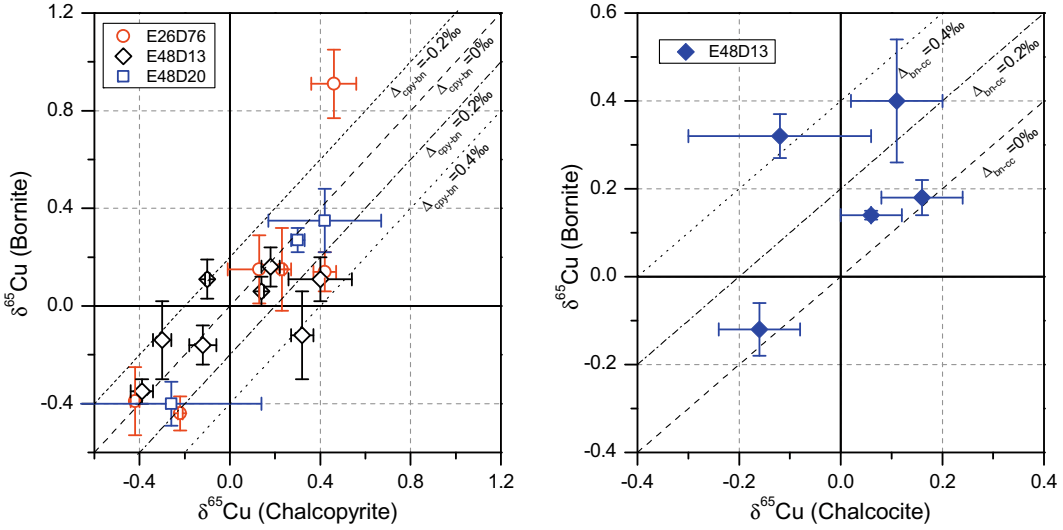

Fig. 6. Plot of δ^{65}Cu values for co-existing sulfides in samples.

is impossible that the depleted Cu isotope zone in each system was produced by simple mixing of the two sources. Therefore, an isotopically evolved hydrothermal fluid is needed to explain the isotopic variation and Cu isotope fractionation must have occurred during the mineralization process to produce such fluid.

Multiple stages of intrusive activity have been identified at Northparkes (Heithersay and Walshe, 1995; Lickfold et al., 2003), with each reflecting a stage in the magmatic evolution of the porphyry system source. For example, the E26 orebody is centered on two quartz monzonite porphyries, QMP1 and the later QMP2. Copper isotope ratios from the two porphyry intrusions are almost the same; the sulfide δ^{65}Cu ranges hosted by QMP1 and QMP2 are 0.18–0.28‰ and 0.13–0.42‰, respectively (sample E26D76-500 m excepted; Fig. 4A). This implies that there is no detectable Cu isotope fractionation during the magmatic activity that produced QMP1 and QMP2. Therefore, the following discussion concentrates on the possible hydrothermal processes that could precipitate sulfides with isotopically light Cu.

5.2.2. Equilibrium isotope fractionation

Equilibrium isotope fractionation is caused by differences in bond energies between different phases for the studied isotopes, with the heavier isotope preferring the higher-energy bond (Schauble, 2004). Copper can exist in three phases in a hydrothermal system: vapor, brine and sulfide. Isotope fractionation due to a difference in bond energies may occur during partitioning of Cu between a brine and a vapor (phase separation), or partitioning of Cu isotopes between hydrothermal fluids and precipitating Cu sulfides. Copper is transported in hydrothermal fluids as Cu(I)-chloride and Cu(I)-bisulfide complexes (e.g., $CuCl_n^{1-n}$ ($n > 1$) and $Cu(HS)_2^-$). Speciation calculations show that chloride complexes are the dominant species of Cu under the conditions prevalent in porphyry systems (Mountain and Seward, 1999, 2003). Evidence from mineral solubility experiments (Xiao et al., 1998; Liu et al., 2001), spectrophotometric (XAFS, XANES, UV) investigations (Fulton et al., 2000a,b; Liu et al., 2002; Brugger et al., 2007) and *ab initio* molecular dynamic simulations (Brugger et al., 2007; Sherman, 2007) reveal that $CuCl_2^-$ is the predominant and stable complex. These studies, together with a quantum mechanics calculation showing that negligible Cu isotopic fractionation occurs between $Cu(HS)_2^-$ and $CuCl_2^-$ in hydrothermal solutions (Seo et al., 2007), imply an absence of Cu isotope fractionation between complex ions in a brine under hydrothermal condition (>300 °C), regardless of the change of temperature and salinity of the brine.

In situ chemical analysis of fluid inclusions has revealed that Cu is preferentially partitioned into the vapor phase rather than the brine (e.g., Heinrich et al., 1999; Williams-Jones and Heinrich, 2005), and that this partitioning is promoted by S (e.g., Simon et al., 2006). Seo et al. (2007) calculated the equilibrium isotope fractionation factors between different Cu(I) species in liquid and vapor between 0 °C and 600 °C and found that both investigated vapor species, Cu_3Cl_3 and $CuCl(H_2O)$, are significantly enriched in ^{65}Cu relative to Cu species in solution, although the possible extent to which this enrichment may be offset by kinetic enrichment of the lighter isotope in the vapor phase has not been tested. Previous fluid inclusion studies reveal that vapor-rich fluid inclusions make up a substantial proportion of the Northparkes fluid inclusion assemblages (Heithersay and Walshe, 1995; Lickfold et al., 2003). If Cu in vapor is isotopically heavier than Cu in solution, as suggested by Seo et al. (2007), outward movement and eventual condensation of a vapor phase and associated Cu as a result of cooling and mixing with meteoric water could have generated the peripheral halo relatively enriched in ^{65}Cu. The substantial associated dilution of the vapor phase Cu and dispersal though the volumetrically predominant peripheral alteration zones would explain the low Cu grades in this region. The brine produced by the boiling (or phase separation) would have been isotopically lighter and this brine could have precipitated Cu at the margin of the orebodies

as a result of the temperature gradient. This could explain the correlation of the low $\delta^{65}Cu$ shells with relatively high Cu grades that then reduce rapidly outwards. The predicted $\Delta^{65}Cu$ between Cu_3Cl_3 (one of the vapor phases of Cu) and $CuCl_2^-$ (the main aqueous phase) is around 0.6‰ at 500 °C and 1.1‰ at 300 °C (Seo et al., 2007). These ranges are comparable with the observed Cu isotope variation from the drill cores (Figs. 4 and 5). Concurrent condensation of acid volatiles at the margin of the orebodies could also explain the transition from K-feldspar to phyllic-dominated alteration that is sometimes associated with these isotopically light zones.

Precipitation of sulfides from hydrothermal fluids is another possible mechanism of Cu isotope fractionation as the bonding conditions of Cu in hydrothermal fluids and sulfides are fundamentally different. Among various physicochemical parameters such as temperature, pH, fO_2 and aCl^-, temperature is the dominant control on Cu solubility in hydrothermal fluids (Herzarkhani et al., 1999). Here, the Cu solubility data from Herzarkhani et al. (1999) is used to generate a Rayleigh fractionation model of the mass and isotopic composition of Cu precipitated from a saturated hydrothermal fluid during cooling with steps of 10 °C (Electronic Annex EA-4). Constant equilibrium isotopic fractionation factors for Cu between hydrothermal fluids and sulfides were used in the calculation and the results of the modeling are shown in Fig. 7A. The influence of temperature on the equilibrium isotopic fractionation factors has been assessed and found to be insignificant (Electronic Annex EA-4). The model shows that, while the amount of precipitated Cu decreases exponentially with temperature, the Cu isotopic compositions of the precipitated sulfides change near linearly with temperature. The linear relationship arises because both the drop in precipitated Cu mass and the concurring isotope fractionation are exponential in a Rayleigh process.

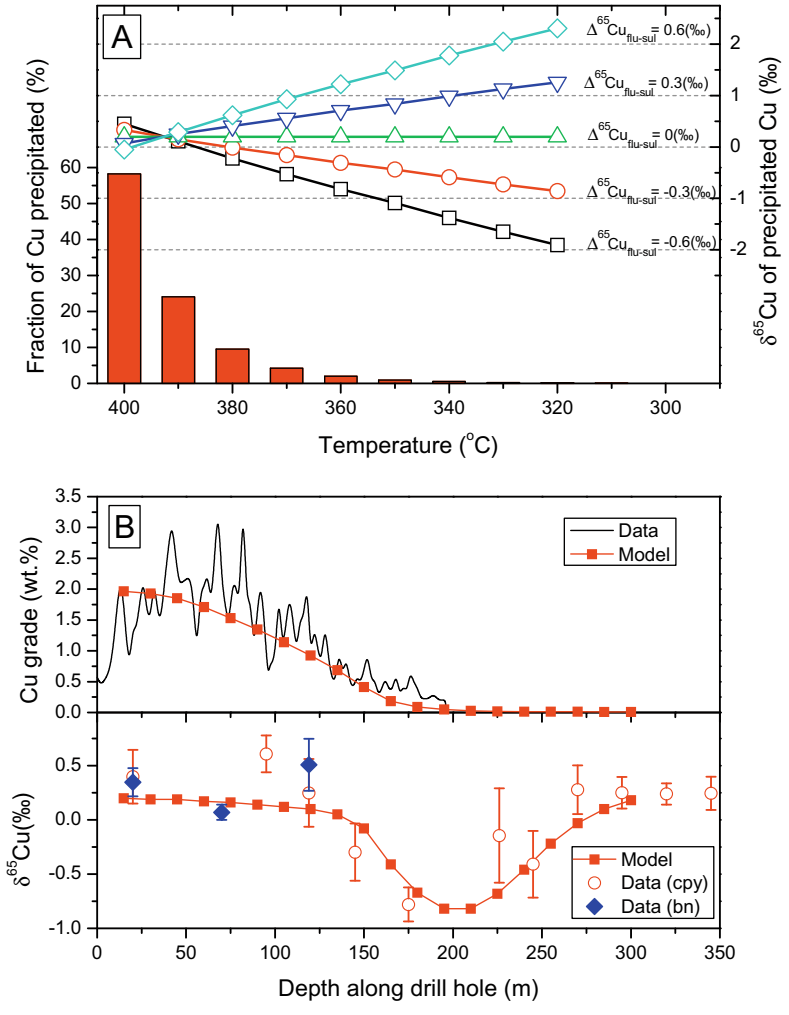

Fig. 7. (A) Plot of fraction of Cu precipitated and the isotopic composition of the precipitated Cu for different fluid–sulfide isotopic fractionation factors as a function of temperature. Solubility data are from Herzarkhani et al. (1999). The assumed $\delta^{65}Cu$ value of the starting fluid is 0.2‰. (B) Plots of modeled and actual profiles of Cu grade and precipitated Cu isotope composition along drill core E48D20. The model assumes a starting hydrothermal fluid with $\delta^{65}Cu$ composition of 0.2‰, a fluid–sulfide isotopic fractionation factor of −0.6‰ and country rocks containing 50 ppm Cu with a $\delta^{65}Cu$ value of 0.2‰. Full details of the modeling are provided in Electronic Annex EA-5.

Although this model is extremely simplified and does not consider any kinetic effects related to sulfide precipitation (e.g., Rouxel et al., 2008), it still provides basic constraints for the interpretation of the observed Cu isotope zonation in the Northparkes deposit. In the classical conceptual model for porphyry ore deposits, a temperature gradient is established between the porphyry intrusions and their host rocks. At Northparkes, the temperature gradient is recorded by the alteration assemblages that change from K-feldspar alteration at the intensively mineralized center to phyllic, propylitic or BMT alterations at the periphery of the porphyry systems, as K-feldspar alteration generally occurs at higher temperature than phyllic and propylitic alterations (e.g., Giggenbach, 1997; Reed and Rusk, 2001; Reed et al., 2005; Cathles and Shannon, 2007). As Cu-bearing fluids permeate outward from the porphyry, they precipitate Cu in response to lowering temperature. Currently no Cu isotope fractionation factors between sulfides and hydrothermal solutions have been published. However, Rouxel et al. (2008) have found that the δ^{56}Fe values of chalcopyrite from black smokers are slightly higher by $0.14 \pm 0.09‰$ than the Fe isotope composition of associated fluids. If the fractionation factor between hydrothermal solution and sulfides ($\Delta^{65}Cu_{fluid-sulfide}$) is negative (^{65}Cu prefers sulfide), the hydrothermal fluid that has undergone Cu precipitation will have a lighter isotopic composition. Then, as the isotopically evolved fluid moves further outward and precipitates Cu due to a further decrease in temperature, the precipitated Cu will have a lighter isotopic composition. To illustrate this, profiles of Cu isotopes and Cu grade along drill core E48D20 have been modeled with a fractionation factor ($\Delta^{65}Cu_{fluid-sulfide}$) of $-0.6‰$ under an equilibrium model with adjustable thermal gradient and multiple fluid releases (see Electronic Annex EA-5 for details). The trends agree well with those observed (Fig. 7B). The rise in δ^{65}Cu from the margin of the ore body to the periphery of the E48 porphyry system is here modeled as homogenization of an isotopically evolved magmatic-hydrothermal Cu (see Fig. 7A) with an outwardly increasing relative proportion of country rock Cu (set as 50 ppm with δ^{65}Cu value of $0.2‰$). However, mixing of the magmatic-hydrothermal fluid with isotopically heavier Cu in a meteoric-hydrothermal fluid would result in a similar trend.

Although there are as yet no published experimental high-temperature $\Delta^{65}Cu_{fluid-sulfide}$ values and smaller fractionation factors would mean that a Rayleigh precipitation process might have contributed less to the lowering in δ^{65}Cu at the margin of the ore body, modeling shows that a Rayleigh-type precipitation–transportation process, coupled with Cu isotope fractionation between hydrothermal fluids and sulfides, is a plausible mechanism for explaining the negative δ^{65}Cu signatures at the margins of the orebodies. The fluid–vapor fractionation and Rayleigh fluid–sulfide fractionation models are compatible with each other and their relative roles cannot be fully evaluated until experimentally determined fractionation factors are available. However, if the former process played only a minor role, an additional explanation is required to explain the most strongly δ^{65}Cu-enriched values in the peripheries of the systems.

5.2.3. Kinetic and redox-related Cu isotope fractionation

Kinetic processes constitute one class of the fundamental mechanisms that produce isotopic fractionation. Diffusion is a kinetic process that could produce isotopic fractionation and this has been used to explain the extremely low δ^{7}Li values around a pegmatite intrusion (Teng et al., 2006). For porphyry systems, however, the diffusion rate of Cu is much slower than the movement of Cu in the hydrothermal fluids that are thought to have been periodically released in surges from a volatile-saturated magma after explosive rupturing of the carapace of the intrusion. And, as significant diffusion of Cu would only have occurred after a Cu concentration gradient was established, any diffusion-driven Cu isotope signatures must have been established after the major mineralizing event associated with the porphyry intrusions. Given that some of the light Cu isotopic signatures occur in rocks that are substantially mineralized (e.g., E26D76-375 m, Figs. 2E and 4A), it seems unlikely that diffusion-related fractionation could have had more than second-order effects on the isotopic signatures.

The most significant isotope fractionations of transition metals are reported in redox processes. Substantial evidence from both laboratory experiments and field samples demonstrate that significant Cu isotope fractionation occur between Cu^{+} and Cu^{2+} (Zhu et al., 2002; Ehrlich et al., 2004; Rouxel et al., 2004; Mathur et al., 2005, 2009; Asael et al., 2006, 2007; Markl et al., 2006; Borrok et al., 2008; Fernandez and Borrok, 2009; Kimball et al., 2009). Cu(I) is the predominant oxidation state for copper under hydrothermal conditions where sulfide is abundant (Mountain and Seward, 1999; Fulton et al., 2000a,b; Liu and McPhail, 2005; Brugger et al., 2007). Cu in hydrothermal fluids and primary sulfides (bornite, chalcopyrite and chalcocite) is also of +1 valence (Goh et al., 2006; Pearce et al., 2006); therefore it is unlikely that redox-related Cu isotope fractionation occurs in the main mineralization stage of porphyry systems.

Redox-related Cu isotope fractionation processes may, however, have played an important role in generating the high δ^{65}Cu signatures at the peripheries of the porphyry systems. The valence of the Cu ion in hydrothermal solutions is mainly controlled by oxygen fugacity, temperature and pH. The ratio of cupric Cu to cuprous Cu or Cu(II)/Cu(I) in solution at different temperatures and oxygen fugacities can be calculated from the reaction:

$$2CuCl^{+} + 2Cl^{-} + H_2O = 2CuCl_2^{-} + 2H^{+} + 0.5O_2$$

$CuCl^{+}$ and $CuCl_2^{-}$ are considered as the representative species of Cu(II) and Cu(I) in typical low-salinity hydrothermal environment (e.g., Collings et al., 2000; Fulton et al., 2000a; Asael et al., 2009). The ratios of Cu(II)/Cu(I) in solution at different temperatures and oxygen fugacities are calculated using a geo-thermodynamic code package SUPCRT92 (Johnson et al., 1992) and the results are plotted in a $\log fO_2$-temperature diagram (Fig. 8). The diagram shows that, Cu(I) is dominant in a hydrothermal solution ($Cu^{2+}/Cu^{+} < 10^{-4}$) under the typical physicochem-

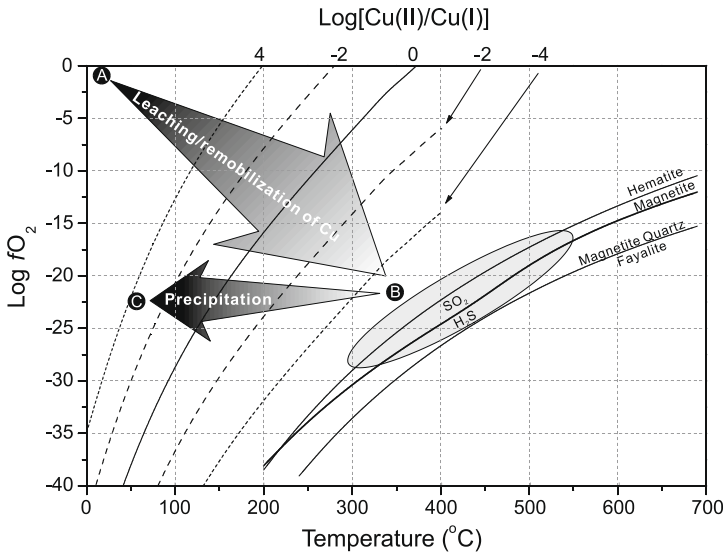

Fig. 8. Plot of predicted trends in oxygen fugacity, temperature and Cu speciation during the convection of groundwater around a porphyry intrusion as discussed in Section 5.2.2. The pH of the solution is set as 4 and the activity of Cl^- is set as −1 to account for the mildly acidic, low-salinity fluid in the periphery of the porphyry system. Thermodynamic properties of $CuCl^+$ and $CuCl_2^-$ are taken from the database of Geochemists' Workbench® as they are not available in the SUPCRT92 database. Points A, B and C represent three different physicochemical conditions attained during the convective cycle. The typical physicochemical conditions for Cu precipitation in porphyry deposits are indicated by the shaded gray oval.

ical conditions for Cu precipitation in porphyry deposits, while Cu(II) is dominant under supergene conditions. These are consistent with observations from natural systems.

Porphyry mineralization is accompanied by fluid convection and circulation around the intrusion (Cathles, 1977). In the first stage of the fluid circulation process, as oxidizing surface water infiltrates downwards and towards the porphyry intrusion, its temperature increases and its oxygen is consumed through fluid–rock interaction (from point A to point B in Fig. 8). The infiltrating fluid oxidizes Cu^+ in the sulfides (and then Cu-rich mafic minerals such as amphibole and biotite) and Cu^{2+} is released into the fluid. This is a redox-related partial leaching process which has been simulated in oxidative leaching experiments conducted by Mathur et al. (2005) which showed that the released Cu^{2+} will be ^{65}Cu-enriched. As revealed in Fig. 8, the valence of the leached isotopically heavy Cu^{2+} gradually changes to +1 as temperature increases and oxygen in the fluid is consumed during its transport towards the intrusion. When the fluid moves away from the porphyry and the temperature drops (from point B to point C in Fig. 8), the isotopically heavy Cu^+ in the solution will be precipitated in response, producing an isotopically heavy halo of Cu around the porphyry intrusion.

Generation of ^{65}Cu-rich groundwaters by near-surface oxidative leaching has been used to explain the high $\delta^{65}Cu$ signatures of sulfide minerals in supergene enrichment zones (Mathur et al., 2009). As described above, the heavy Cu isotopic signatures of sulfides from the periphery of the E48 and E26 systems can also be explained by redox reactions during remobilization–precipitation processes related to convecting meteoric water, perhaps together with condensed isotopically heavy Cu from Cu-rich vapor that is diluted and dispersed by the meteoric water in the periphery of the systems. The redox model is compatible with the interpretation for Cu isotopic variation in sea-floor hydrothermal systems (Rouxel et al., 2004), and may also be able to explain the heavy Cu isotope compositions of sulfides in distal skarn deposits (Graham et al., 2004; Maher and Larson, 2007) and some abnormal Cu isotope signatures found in granites (Li et al., 2009).

5.3. Decoupling of isotopic fractionation of S and Fe from Cu

Sulfur isotopic data from drill cores E26D76 and E48D20 show systematic variations around the orebodies. Bornite samples from the most intensely mineralized rocks (QMP1) of the E26 orebody have the highest $\delta^{34}S$ value (core depth between 600 m and 700 m along drill core E26D76). Samples from the later and less mineralized QMP2 and periphery of the E26 orebody are isotopically lighter. Samples from the E48 orebody show a similar pattern, with S isotopic data for samples from the center of the orebody having the highest $\delta^{34}S$ values. There are zones of isotopically light S on both sides of the deposit but these occur outward from the zones of light Cu isotope signatures. The S isotope data of this study confirm the finding of Heithersay and Walshe (1995), who reported that the $\delta^{34}S$ value of bornite from the core of the E26 orebody was ca. −3‰, and the isotopic compositions of sulfides grading out laterally and vertically dropped to −8‰.

H_2S and SO_2 are the predominant sulfur species in high-temperature (>400 °C) hydrothermal fluids. At temperatures below 400 °C, SO_2 will disproportionate according to the reaction $4SO_2 + 4H_2O = 3H_2SO_4 + H_2S$. Nevertheless, ^{34}S is depleted in sulfides relative to an associated hydrothermal fluid and the equilibrium sulfur isotope fractionation factor between the oxidized sulfur species (sulfates) and reduced

sulfur species (sulfides) increases with decreasing temperature (Ohmoto and Rye, 1979). Modeling shows that the $\delta^{34}S$ values of precipitated sulfides from a common source decrease with cooling, irrespective of whether the fluid is oxidizing or reducing (Rye, 1993; Wilson et al., 2007). Therefore, the lower $\delta^{34}S$ values of sulfides from the margins of orebodies are consistent with precipitation at lower temperatures than sulfides from the center of orebody. This is in accord with the general understanding of the physical conditions of the porphyry systems and is consistent with the "equilibrium model" for the observed Cu isotope fractionation.

It should be noted that the decrease in $\delta^{34}S$ values away from the porphyry system is not monotonic. In drill core E48D20, the $\delta^{34}S$ values increase in sulfides from the outer periphery of the ore system (Fig. 5A). Lickfold (2002) compiled all the available S isotope data from the Northparkes deposit and found a similar trend of S isotope variation, with an overall increase in $\delta^{34}S$ outward in the periphery of the porphyry systems. This trend is also reported from the propylitic halos of the porphyry Au–Cu deposits of the Cadia district, which are also located in the Lachlan Fold Belt of central New South Wales, Australia (Wilson et al., 2007). This trend of increasing sulfide $\delta^{34}S$ is explained by reduction of sulfate during propylitic alteration at temperatures around 200–350 ℃ (Wilson et al., 2007).

Plots of $\delta^{65}Cu$ and $\delta^{34}S$ values from the same samples from the two orebodies show no systematic correlation between the two isotope systems (Fig. 9). This is probably because of the different geochemical behavior of S and Cu in porphyry systems. Sulfur has two different species (SO_2 and H_2S) at high temperature, and there is strong equilibrium isotopic fractionation between the two. By contrast, Cu has only one main species in high-temperature hydrothermal solutions, and significant isotopic fractionation between Cu species only occurs in oxidized low-temperature hydrothermal fluids. Rouxel et al. (2004) also found no systematic relationship between the $\delta^{34}S$ and $\delta^{65}Cu$ data from black smokers, and proposed that while Cu isotopes are fractionated during sulfide–fluid interaction and surface/subsurface redox processes, S isotopes are fractionated by seawater sulfate reduction and leaching of volcanic rocks. The decoupling of the S and Cu isotopic systems provides geochemists and economic geologists with a powerful tool for discerning the physicochemical conditions of different hydrothermal processes.

Iron is also a major component in many sulfides, and its isotopes are sensitive to redox change (Poitrasson and Freydier, 2005; Teng et al., 2008) even at high temperature. Iron isotopic compositions of chalcopyrite in drill core E26D76 were analyzed in the previous reconnaissance industry research project with LA-MC-ICP-MS (Graham et al., 2002). The results are plotted in Fig. 4B. $\delta^{57}Fe$ values of chalcopyrite all cluster around 0‰ (relative to IRMM-014 Fe isotopic standard) and show no correlation with $\delta^{65}Cu$ values, Cu grade or alteration assemblage. The decoupling of Cu and Fe isotope data may be a result of one or more of the following: (1) while Cu partitions strongly into a vapor phase during boiling, a process that is predicted to result in significant Cu isotope fractionation (Seo et al, 2007), Fe preferentially partitions into the brine (Heinrich et al., 1999; Williams-Jones and Heinrich, 2005); (2) Fe is a major element in rocks and can thus be released in abundance during hydrothermal alteration; Rayleigh fractionation processes do not, therefore, apply to Fe isotopes due to the reservoir effect and (3) the redox potential for the Cu^{2+}/Cu^{+} couple is much lower than the Fe^{3+}/Fe^{2+} couple (Albarède, 2004); therefore Cu isotopes are more sensitive to redox processes which may have occurred in the peripheries of the porphyry systems.

Graham et al. (2004) observed distinct differences in Fe isotopic compositions between the sulfides from the igneous intrusion of the Grasberg porphyry and chalcopyrite from the Pyrite Shell enveloping the Cu–Au mineralization. They suggested that the Fe in the Pyrite Shell is a mixture between sedimentary and igneous sources. By con-

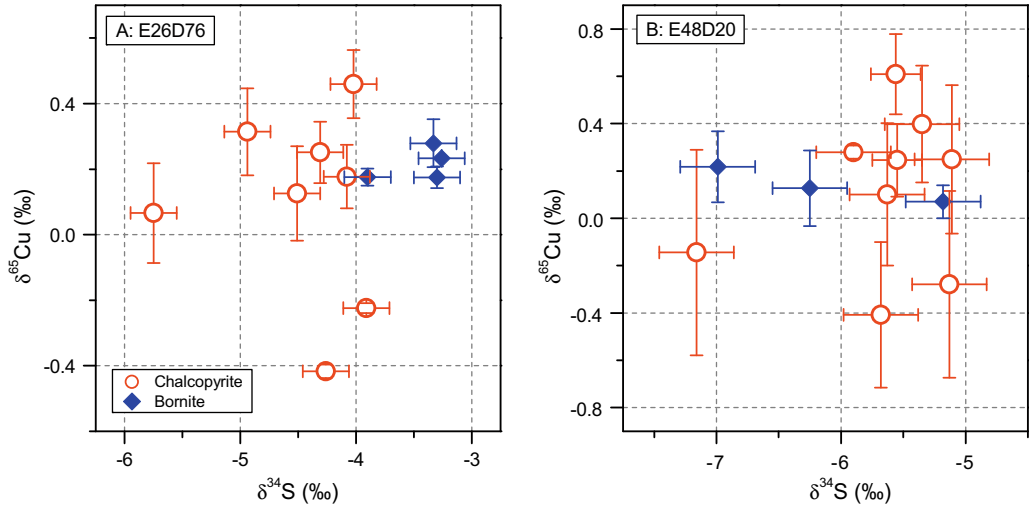

Fig. 9. Plot of $\delta^{65}Cu$ versus $\delta^{34}S$ values for samples from the E26 and E48 orebodies.

trast, the tight clustering of δ^{57}Fe values of chalcopyrite in drill core E26D76 supports an orthomagmatic origin for the E26 ore.

This study showcases the power of integrating the S–Cu–Fe isotopic systems to provide multiple constraints on the source of ore-forming elements and mineralization processes; this will prove valuable in ore deposit research.

5.4. Implications for mineral exploration

The equilibrium model presented in Section 5.2.2 describes the Cu isotope response to the temperature-sensitive ore-forming process, and bears some important implications in application of Cu isotope in high-temperature hydrothermal deposits. Firstly, at the beginning of this Rayleigh-type process, the isotopic fractionation is not magnified. As the solubility of Cu drops exponentially with temperature, the majority of the Cu is precipitated in a small temperature interval and, by and large, this Cu preserves the isotopic composition of the source (Fig. 7A). Therefore, the Cu isotopic composition of the intensely mineralized core of the orebody provides an estimate of the composition of the source fluids. Secondly, Cu is a fluid mobile element that can be transported far from its source and precipitated in rocks in which Cu concentration anomaly and hydrothermal alteration are not significantly developed. However, this evolved Cu may bear strongly fractionated Cu isotope signatures (Fig. 7) and impart a significant Cu isotope anomaly on the rock (Li et al., 2009). Copper isotopes may therefore be a sensitive exploration tool for fingerprinting distal hydrothermal activity potentially associated with more significant mineralization at depth.

6. CONCLUDING REMARKS

Accurate and precise measurement of the isotopic composition of Cu-bearing sulfides with laser ablation MC-ICP-MS and solution MC-ICP-MS after microdrilling has been achieved in this study. Significant Cu isotope variation (from $-1.67‰$ to $0.85‰$ in δ^{65}Cu) is found in the high temperature, orthomagmatic Northparkes porphyry Cu deposit. The LA-MC-ICP-MS analysis has revealed Cu isotopic heterogeneity of samples on the hand specimen scale. However, this variation is of second order compared to Cu isotopic variation on the deposit scale.

Based on the Cu isotopic analyses on samples from four drill cores crosscutting two different porphyry systems from different directions, systematic Cu isotopic zonation in the porphyry systems of the Northparkes district is revealed. The sulfides in the high-grade cores of two porphyry orebodies have a Cu isotopic composition of around $0.2‰$ ($0.19 \pm 0.14‰$, 1σ, $n = 40$) in δ^{65}Cu. At the margins of the orebody, where Cu grade decreases rapidly outward, the δ^{65}Cu of sulfides drops to $-0.4‰$ ($-0.25 \pm 0.36‰$, 1σ, $n = 30$) before increasing to outwards to 0.4–0.8‰ ($0.29 \pm 0.56‰$, 1σ, $n = 20$) in the periphery of the porphyry systems.

The Cu isotopic variation may be caused by the isotopic fractionation of Cu between brine, sulfide and vapor during the porphyry mineralization processes including sulfide precipitation from brine in response to temperature decrease and boiling. Other mechanisms, such as kinetic isotope and redox-related Cu isotope fractionation, are less likely to account for the Cu isotope variation in the ore zones of the Northparkes deposits, although redox-related Cu isotope fractionation may have played a role in producing the high δ^{65}Cu signatures in the periphery of the orebodies. Therefore, Cu isotopes may be useful for fingerprinting hydrothermal processes. As Cu isotopes in the distal zones of porphyry systems are most strongly fractionated, they may also be useful in mineral exploration for fingerprinting cryptic hydrothermal activity.

This study discusses the possible processes to explain the observed Cu isotopic zonation from the Northparkes deposit; however, quantitative estimation of the relative contributions of the different Cu isotope fractionation processes is not made. Significant gaps remain in our knowledge of Cu isotope fractionation in high-temperature hydrothermal systems. The most significant ones are the direction and magnitude of Cu isotope fractionation between vapor, brine and sulfides during boiling of supercritical fluid released from the magma and during hydrothermal precipitation. More theoretical modeling, experimental determinations, and natural system investigations are needed in order to make Cu isotope a mature tool for mineral deposit studies.

ACKNOWLEDGMENTS

This study is a part of Ph.D. project (W. Li), and was financially supported by ARC Discovery Grant (DP0557779) to S.E. Jackson. The analytical data were obtained using instrumentation funded by ARC LIEF, and DEST, Systemic Infrastructure Grants, industry partners and Macquarie University. We thank Mr. Peter Wieland and Ms. Suzy Elhlou for assistance in lab work. Northparkes Mines provided logistical support during sampling, and access to Cu grade data of the four drill cores and internal industry reports. Drs. R. Mathur, A. Matthews, O. Rouxel and an anonymous reviewer are thanked for their constructive criticisms. This is publication no. 631 from the GEMOC ARC National Key Centre, www.es.mq.edu.au/GEMOC/.

APPENDIX A. SUPPLEMENTARY DATA

Supplementary data associated with this article can be found, in the online version, at doi:10.1016/j.gca.2010.04.003.

REFERENCES

Albarède F. (2004) The stable isotope geochemistry of copper and zinc. *Rev. Mineral. Geochem.* **55**(1), 409–427.

Archer C. and Vance D. (2004) Mass discrimination correction in multiple-collector plasma source mass spectrometry: an example using Cu and Zn isotopes. *J. Anal. At. Spectrom.* **19**, 656–665.

Asael D., Matthews Butler I., Rickard A. D., Bar-Matthews M. and Halicz L. (2006) ^{65}Cu/^{63}Cu fractionation during copper sulphide formation from iron sulphides in aqueous solution. *Geochim. Cosmochim. Acta* **70**(18), A23.

Asael D., Matthews A., Bar-Matthews M. and Halicz L. (2007) Copper isotope fractionation in sedimentary copper mineralization (Timna Valley, Israel). *Chem. Geol.* **243**(3–4), 238–254.

Asael D., Matthews A., Oszczepalski S., Bar-Matthews M. and Halicz L. (2009) Fluid speciation controls of low temperature copper isotope fractionation applied to the Kupferschiefer and Timna ore deposits. *Chem. Geol.* **262**(3–4), 147–158.

Borrok D. M., Nimick D. A., Wanty R. B. and Ridley W. I. (2008) Isotopic variations of dissolved copper and zinc in stream waters affected by historical mining. *Geochim. Cosmochim. Acta* **72**(2), 329–344.

Brugger J., Etschmann B., Liu W., Testemale D., Hazemann J. L., Emerich H., van Beek W. and Proux O. (2007) An XAS study of the structure and thermodynamics of Cu(I) chloride complexes in brines up to high temperature (400 ℃, 600 bar). *Geochim. Cosmochim. Acta* **71**(20), 4920–4941.

Butera K. M., Williams I. S., Blevin P. L. and Simpson C. J. (2001) Zircon U–Pb dating of Early Palaeozoic monzonitic intrusives from the Goonumbla area, New South Wales. *Aust. J. Earth Sci.* **48**(3), 457–464.

Cathles L. M. (1977) An analysis of the cooling of intrusives by ground-water convection which includes boiling. *Econ. Geol.* **72**, 804–826.

Cathles L. M. and Shannon R. (2007) How potassium silicate alteration suggests the formation of porphyry ore deposits begins with the nearly explosive but barren expulsion of large volumes of magmatic water. *Earth Planet. Sci. Lett.* **262**(1–2), 92–108.

Charlier B. L. A., Ginibre C., Morgan D., Nowell G. M., Pearson D. G., Davidson J. P. and Ottley C. J. (2006) Methods for the microsampling and high-precision analysis of strontium and rubidium isotopes at single crystal scale for petrological and geochronological applications. *Chem. Geol.* **232**(3–4), 114–133.

Collings M. D., Sherman D. M. and Ragnarsdottir K. V. (2000) Complexation of Cu^{2+} in oxidized NaCl brines from 25 °C to 175 °C: results from in situ EXAFS spectroscopy. *Chem. Geol.* **167**(1–2), 65–73.

Ehrlich S., Butler I., Halicz L., Rickard D., Oldroyd A. and Matthews A. (2004) Experimental study of the copper isotope fractionation between aqueous Cu(II) and covellite, CuS. *Chem. Geol.* **209**(3–4), 259–269.

Farmer G. L. and DePaolo D. J. (1997) Sources of hydrothermal components: heavy isotopes. In *Geochemistry of Hydrothermal Ore Deposits* (ed. H. L. Barnes). John Wiley & Sons, pp. 31–61.

Fernandez A. and Borrok D. M. (2009) Fractionation of Cu, Fe, and Zn isotopes during the oxidative weathering of sulfide-rich rocks. *Chem. Geol.* **264**(1–4), 1–12.

Fulton J. L., Hoffmann M. M. and Darab J. G. (2000a) An X-ray absorption fine structure study of copper(I) chloride coordination structure in water up to 325℃. *Chem. Phys. Lett.* **330**(3–4), 300–308.

Fulton J. L., Hoffmann M. M., Darab J. G., Palmer B. J. and Stern E. A. (2000b) Copper(I) and copper(II) coordination structure under hydrothermal conditions at 325℃: an X-ray absorption fine structure and molecular dynamics study. *J. Phys. Chem. A* **104**(49), 11651–11663.

Giggenbach W. F. (1997) The origin and evolution of fluids in magmatic-hydrothermal systems. In *Geochemistry of Hydrothermal Ore Deposits* (ed. H. L. Barnes). John Wiley & Sons, pp. 737–796.

Goh S. W., Buckley A. N., Lamb R. N., Rosenberg R. A. and Moran D. (2006) The oxidation states of copper and iron in mineral sulfides, and the oxides formed on initial exposure of chalcopyrite and bornite to air. *Geochim. Cosmochim. Acta* **70**(9), 2210–2228.

Graham S., Jackson S. and Griffin W. (2002) Isotopic composition of Cu and Fe in ore minerals. In *Unpublished Final Report of Macquarie University External Collaborative Research Grant A002888*. Macquarie University, pp. 1–70.

Graham S., Pearson N., Jackson S., Griffin W. and O'Reilly S. Y. (2004) Tracing Cu and Fe from source to porphyry: in situ determination of Cu and Fe isotope ratios in sulfides from the Grasberg Cu–Au deposit. *Chem. Geol.* **207**(3–4), 147–169.

Halliday A. N., Lee D. C., Christensen J. N., Rehkamper M., Yi W., Luo X. Z., Hall C. M., Ballentine C. J., Pettke T. and Stirling C. (1998) Applications of multiple collector-ICPMS to cosmochemistry, geochemistry, and paleoceanography. *Geochim. Cosmochim. Acta* **62**(6), 919–940.

Harris A. C. and Golding S. D. (2002) New evidence of magmatic-fluid-related phyllic alteration: implications for the genesis of porphyry Cu deposits. *Geology* **30**(4), 335–338.

Hedenquist J. W. and lowenstern J. B. (1994) The role of magmas in the formation of hydrothermal ore deposits. *Nature* **370**, 519–527.

Heinrich C. A., Gunther D., Audetat A., Ulrich T. and Frischknecht R. (1999) Metal fractionation between magmatic brine and vapor, determined by microanalysis of fluid inclusions. *Geology* **27**(8), 755–758.

Heithersay P. S. and Walshe J. L. (1995) Endeavour 26 North: a porphyry copper–gold deposit in the Late Ordovician shoshonitic Goonumbla Volcanic Complex, NSW, Australia. *Econ. Geol.* **90**, 1506–1532.

Heithersay P. S., O'Neill W. J., van der Helder P., Moore C. R., Harbon P. G. and Hughes F. E. (1990) Goonumbla porphyry copper district—endeavour 26 north, endeavour 22 and endeavour 27 copper–gold deposits. In *Geology of the Mineral Deposits of Australia and Papua New Guinea*. Australian Institute of Mining and Metallurgy, pp. 1385–1398.

Herzarkhani A., Williams-Jones A. E. and Gammons C. H. (1999) Factors controlling copper solubility and chalcopyrite deposition in the Sungun porphyry copper deposit, Iran. *Miner. Deposita* **34**(8), 770–783.

Howland-Rose J. S. (1996) Fluid evolution at the endeavour 48 porphyry Cu–Au deposit, Parkes, NSW. Unpublished B.Sc. honours thesis, The University of Newcastle.

Ikehata K., Notsu K. and Hirata T. (2008) In situ determination of Cu isotope ratios in copper-rich materials by NIR femtosecond LA-MC-ICP-MS. *J. Anal. At. Spectrom.* **23**(7), 1003–1008.

Jackson S. E. and Günther D. (2003) The nature and sources of laser induced isotopic fractionation in laser ablation-multicollector-inductively coupled plasma-mass spectrometry. *J. Anal. At. Spectrom.* **18**(3), 205–212.

Jiang S., Woodhead J., Yu J., Pan J., Liao Q. and Wu N. (2002) A reconnaissance study of Cu isotopic compositions of hydrothermal vein-type copper deposit, Jinman, Yunan, China. *Chin. Sci. Bull.* **47**(3), 247–250.

Johnson J. W., Oelkers E. H. and Helgeson H. C. (1992) SUPCRT92: a software package for calculating the standard molal thermodynamic properties of minerals, gases, aqueous species, and reactions from 1 to 5000 bar and 0 to 1000℃. *Comput. Geosci.* **18**(7), 899–947.

Jones G. J. (1985) The Goonumbla porphyry copper deposits, New South Wales. *Econ. Geol.* **80**, 591–613.

Jones B. M. (1991) Geological setting and genesis of the endeavour 44 Au, Pb, Zn skarn, Parkes, NSW. B.Sc. honours thesis, Australian National University.

Kimball B. E., Mathur R., Dohnalkova A. C., Wall A. J., Runkel R. L. and Brantley S. L. (2009) Copper isotope fractionation in acid mine drainage. *Geochim. Cosmochim. Acta* **73**(5), 1247–1263.

Kühn H. R., Pearson N. J. and Jackson S. E. (2007) The influence of the laser ablation process on isotopic fractionation of copper in LA-MC-ICP-MS. *J. Anal. At. Spectrom.* **22**(5), 547–552.

Larson P. B., Maher K., Ramos F. C., Chang Z. S., Gaspar M. and Meinert L. D. (2003) Copper isotope ratios in magmatic and hydrothermal ore-forming environments. *Chem. Geol.* **201**(3–4), 337–350.

Li W.-Q., Jackson S. E., Pearson N. J., Alard O. and Chappell B. W. (2009) The Cu isotopic signature of granites from the Lachlan Fold Belt, SE Australia. *Chem. Geol.* **258**, 38–49.

Lickfold V. (2002) Intrusive history and volatile evolution of the endeavour porphyry Cu–Au deposits, Goonumbla District, NSW, Australia. Ph.D. thesis, University of Tasmania.

Lickfold V., Cooke D. R., Smith S. G. and Ullrich T. D. (2003) Endeavour copper–gold porphyry deposits, Northparkes, New South Wales: intrusive history and fluid evolution. *Econ. Geol. Bull. Soc. Econ. Geol.* **98**(8), 1607–1636.

Liu W. H. and McPhail D. C. (2005) Thermodynamic properties of copper chloride complexes and copper transport in magmatic-hydrothermal solutions. *Chem. Geol.* **221**(1–2), 21–39.

Liu W., McPhail D. C. and Brugger J. (2001) An experimental study of copper(I)-chloride and copper(I)-acetate complexing in hydrothermal solutions between 50°C and 250°C and vapor-saturated pressure. *Geochim. Cosmochim. Acta* **65**(17), 2937–2948.

Liu W., Brugger J., McPhail D. C. and Spiccia L. (2002) A spectrophotometric study of aqueous copper(I)-chloride complexes in LiCl solutions between 100°C and 250°C. *Geochim. Cosmochim. Acta* **66**(20), 3615–3633.

Lowell J. D. and Guilbert J. M. (1970) Lateral and vertical alteration–mineralisation zoning in porphyry ore deposits. *Econ. Geol.* **65**, 373–408.

Maher K. C. and Larson P. B. (2007) Variation in copper isotope ratios and controls on fractionation in hypogene skarn mineralization at Coroccohuayco and Tintaya, Peru. *Econ. Geol.* **102**(2), 225–237.

Maréchal C. N., Télouk P. and Albarède F. (1999) Precise analysis of copper and zinc isotopic compositions by plasma-source mass spectrometry. *Chem. Geol.* **156**(1–4), 251–273.

Markl G., Lahaye Y. and Schwinn G. (2006) Copper isotopes as monitors of redox processes in hydrothermal mineralization. *Geochim. Cosmochim. Acta* **70**(16), 4215–4228.

Mason T. F. D., Weiss D. J., Chapman J. B., Wilkinson A. J., Tessalina V. G., Spiro A., Horstwood A. S. A., Spratt O. and Coles A. J. (2005) Zn and Cu isotopic variability in the Alexandrinka volcanic-hosted massive sulphide (VHMS) ore deposit, Urals, Russia. *Chem. Geol.* **221**, 170–187.

Mathur R., Ruiz J., Titley S., Gibbins S. and Margotomo W. (2000) Different crustal sources for Au-rich and Au-poor ores of the Grasberg Cu–Au porphyry deposit. *Earth Planet. Sci. Lett.* **183**(1–2), 7–14.

Mathur R., Ruiz J., Titley S., Liermann L., Buss H. and Brantley S. (2005) Cu isotopic fractionation in the supergene environment with and without bacteria. *Geochim. Cosmochim. Acta* **69**(22), 5233–5246.

Mathur R., Titley S., Barra F., Brantley S., Wilson M., Phillips A., Munizaga F., Maksaev V., Vervoort J. and Hart G. (2009) Exploration potential of Cu isotope fractionation in porphyry copper deposits. *J. Geochem. Explor.* **102**(1), 1–6.

Mountain B. W. and Seward T. M. (1999) The hydrosulphide/sulphide complexes of copper(I): experimental determination of stoichiometry and stability at 22°C and reassessment of high temperature data. *Geochim. Cosmochim. Acta* **63**(1), 11–29.

Mountain B. W. and Seward T. M. (2003) Hydrosulfide/sulfide complexes of copper(I): experimental confirmation of the stoichiometry and stability of $Cu(HS)_2^-$ to elevated temperatures. *Geochim. Cosmochim. Acta* **67**(16), 3005–3014.

Ohmoto H. and Rye R. O. (1979) Isotopes of sulfur and carbon. In *Geochemistry of Hydrothermal Ore Deposits* (ed. H. L. Barnes). John Wiley & Sons, pp. 509–567.

Pearce C. I., Pattrick R. A. D., Vaughan D. J., Henderson C. M. B. and van der Laan G. (2006) Copper oxidation state in chalcopyrite: mixed Cu d^9 and d^{10} characteristics. *Geochim. Cosmochim. Acta* **70**(18), 4635–4642.

Perkins C., McDougall I., Claoue-Long J. and Heithersay P. S. (1990) $^{40}Ar/^{39}Ar$ and U–Pb geochronology of the Goonumbla porphyry Cu–Au deposits, New South Wales, Australia. *Econ. Geol.* **85**(8), 1808–1824.

Poitrasson F. and Freydier R. (2005) Heavy iron isotope composition of granites determined by high resolution MC-ICP-MS. *Chem. Geol.* **222**(1–2), 132–147.

Reed M. H. and Rusk B. (2001) Insights into supercritical hydrothermal processes from numerical models of potassic hydrothermal alteration, and SEM-CL imaging of vein quartz at Butte, Montana. In *Proceedings from the Workshop on Potential Thermal Extraction from Deep-Seated Rock Masses* (ed. H. Toshiyuki). Tohoku University, pp. 37–53.

Reed M. H., Rusk B., Palandri J. and Dilles J. (2005) The Butte hydrothermal system: one magmatic fluid yielded all vein types. *Geol. Soc. Am. Abstr. Programs* **37**(7), A315.

Rouxel O., Fouquet Y. and Ludden J. N. (2004) Copper isotope systematics of the Lucky Strike, Rainbow, and Logatchev sea-floor hydrothermal fields on the Mid-Atlantic Ridge. *Econ. Geol. Bull. Soc. Econ. Geol.* **99**(3), 585–600.

Rouxel O., Shanks Iii W. C., Bach W. and Edwards K. J. (2008) Integrated Fe- and S-isotope study of seafloor hydrothermal vents at East Pacific Rise 9–10°N. *Chem. Geol.* **252**(3–4), 214–227.

Rye R. O. (1993) The evolution of magmatic fluids in the epithermal environment: the stable isotope perspective. *Econ. Geol.* **88**(3), 733–752.

Schauble E. A. (2004) Applying stable isotope fractionation theory to new systems. In *Geochemistry of Non-Traditional Stable Isotopes*, vol. 55. Mineralogical Society of America, pp. 65–111.

Seo J. H., Lee S. K. and Lee I. (2007) Quantum chemical calculations of equilibrium copper(I) isotope fractionations in ore-forming fluids. *Chem. Geol.* **243**(3–4), 225–237.

Sheppard S. M. F. and Gustafson L. (1976) Oxygen and hydrogen isotopes in the porphyry copper deposit at El Salvador, Chile. *Econ. Geol.* **71**, 1549–1559.

Sherman D. M. (2007) Complexation of Cu^+ in hydrothermal NaCl brines: ab initio molecular dynamics and energetics. *Geochim. Cosmochim. Acta* **71**(3), 714–722.

Shields W. R., Goldich S. S., Garner E. L. and Murphy T. J. (1965) Natural variations in the abundance ratios and the atomic weight of copper. *J. Geophys. Res.* **70**(2), 479–491.

Simon A. C., Pettke T., Candela P. A., Piccoli P. M. and Heinrich C. A. (2006) Copper partitioning in a melt–vapor–brine–magnetite–pyrrhotite assemblage. *Geochim. Cosmochim. Acta* **70**(22), 5583–5600.

Simpson C. J., Cas R. A. F. and Arundell M. C. (2005) Volcanic evolution of a long-lived Ordovician island-arc province in the Parkes region of the Lachlan Fold Belt, southeastern Australia. *Aust. J. Earth Sci.* **52**(6), 863–886.

Suppel D. W., Barnes R. G. and Scheibner E. (1998) The Palaeozoic in New South Wales: geology and mineral resources. *AGSO J. Aust. Geol. Geophys.* **17**(3), 87–105.

Teng F.-Z., McDonough W. F., Rudnick R. L. and Walker R. J. (2006) Diffusion-driven extreme lithium isotopic fractionation in country rocks of the Tin Mountain pegmatite. *Earth Planet. Sci. Lett.* **243**(3–4), 701–710.

Teng F. Z., Dauphas N. and Helz R. T. (2008) Iron isotope fractionation during magmatic differentiation in Kilauea Iki Lava Lake. *Science* **320**(5883), 1620–1622.

Walder A. J. (1997) Advanced isotope ratio mass spectrometry II: isotope ratio measurement by multiple collector inductively coupled plasma mass spectrometry. In *Modern Isotope Ratio Mass Spectrometry* (ed. I. T. Platzner). John Wiley & Sons, pp. 83–108.

Walder A. J., Platzner I. and Freedman P. A. (1993) Isotope ratio measurement of lead, neodymium and neodymium–samarium mixtures, hafnium and hafnium–lutetium mixtures with a double focusing multiple collector inductively coupled plasma mass spectrometer. *J. Anal. At. Spectrom.* **8**, 19–23.

Walker E. C., Cuttitta F. and Senftle F. E. (1958) Some natural variations in the relative abundance of copper isotopes. *Geochim. Cosmochim. Acta* **15**, 183–194.

Williams-Jones A. E. and Heinrich C. A. (2005) 100th anniversary special paper: vapor transport of metals and the formation of magmatic-hydrothermal ore deposits. *Econ. Geol.* **100**(7), 1287–1312.

Wilson A., Cooke D., Harper B. and Deyell C. (2007) Sulfur isotopic zonation in the Cadia district, southeastern Australia: exploration significance and implications for the genesis of alkalic porphyry gold–copper deposits. *Miner. Deposita* **42**(5), 465–487.

Xiao Z., Gammons C. H. and Williams-Jones A. E. (1998) Experimental study of copper(I) chloride complexing in hydrothermal solutions at 40 to 300°C and saturated water vapor pressure. *Geochim. Cosmochim. Acta* **62**(17), 2949–2964.

Zhu X. K., O'Nions R. K., Guo Y., Belshaw N. S. and Rickard D. (2000) Determination of natural Cu-isotope variation by plasma-source mass spectrometry: implications for use as geochemical tracers. *Chem. Geol.* **163**(1–4), 139–149.

Zhu X. K., Guo Y., Williams R. J. P., O'Nions R. K., Matthews A., Belshaw N. S., Canters G. W., de Waal E. C., Weser U., Burgess B. K. and Salvato B. (2002) Mass fractionation processes of transition metal isotopes. *Earth Planet. Sci. Lett.* **200**(1–2), 47–62.

Associate editor: Edward M. Ripley